BIOCONVECTION IN REINER-PHILIPPOFF FLUID FLOW OVER A SLENDERING SHEET

Thesis Submitted By

SABA NOUREEN

(01-248202-008)

Supervised By

Dr. Jafar Hasnain

Department of Computer Science

Bahria University Islamabad, Pakistan

2022

BIOCONVECTION IN REINER-PHILIPPOFF FLUID FLOW OVER A SLENDERING SHEET

Thesis Submitted By

SABA NOUREEN

(01-248202-008)

Supervised By

Dr. Jafar Hasnain

A thesis submitted in fulfilment of the requirements for the award of degree of Master of Science (Computer Science)

Department of Computer Science
BAHRIA UNIVERSITY ISLAMABAD

OCTOBER 2022

Approval of Examination

Scholar Name: Saba Noureen
Registration Number: 71099
Enrollment: 01-248202-008
Program of Study: MS Mathematics

Thesis Title: “Bioconvection in Reiner-Philippoff fluid flow over a slendering sheet”

It is to certify that the above scholar’s thesis has been completed to my satisfaction and, to my belief, its standard is appropriate for submission for examination. I have also conducted plagiarism test of this thesis using HEC prescribed software and found similarity index 18%. that is within the permissible limit set by the HEC for the MS/M. Phil degree thesis. I have also found the thesis in a format recognized by the BU for the MS/M.Phil thesis.

Supervisor Name: Dr. Jafar Hasnain

Supervisor Signature:

Date:

Author's Declaration

I, Saba Noureen hereby state that my MS/M.Phil thesis titled is my own work and has not been submitted previously by me for taking any degree from Bahria university or anywhere else in the country/world. At any time if my statement is found to be incorrect even after my graduation, the University has the right to withdraw/cancel my MS/M.Phil degree.

Scholar signature: _____

Name of Scholar: SABA NOUREEN

Date: 21-11-2022

Plagiarism Undertaking

I, Saba Noureen solemnly declare that research work presented in the thesis titled "Bioconvection in Reiner-Philippoff fluid flow over a slendering sheet" is solely my research work with no significant contribution from any other person. Small contribution / help wherever taken has been duly acknowledged and that complete thesis has been written by me. I understand the zero-tolerance policy of the HEC and Bahria University towards plagiarism. Therefore, I as an Author of the above titled thesis declare that no portion of my thesis has been plagiarized and any material used as reference is properly referred / cited.

I undertake that if I am found guilty of any formal plagiarism in the above titled thesis even after award of MS/M.Phil degree, the university reserves the right to withdraw / revoke my MS/M.Phil degree and that HEC and the University has the right to publish my name on the HEC / University website on which names of scholars are placed who submitted plagiarized thesis

Name of Scholar: SABA NOUREEN

Date: 21-11-2022

Dedication

I dedicate this thesis to my beloved mother because whatever I am is due to my mother's hard work whose prays, love and endless support have been a source of inspiration and encouragement for me.

I also dedicate this thesis to my respected supervisor Dr. Jafar Hasnain who has intellectually accompanied me in my research inquiry and impressed me with this hard work and sincerity

Acknowledgments

Everlasting praise to ALLAH Almighty the most gracious, the most merciful who bestowed me with His great blessings. I am really blessed as He gave me the ability to think even upon a little tiny thing He created. He gave me a source (His beloved PROPHET (PBUH)) of light for my way to Him.

I would like to express my sincere gratitude to my kind mentor and supervisor Dr. Jafar Hasnain for his persistent, continuous, dedicated, and pertinent guidance that kept me motivated to complete my thesis. It has been an honor to have him as my supervisor for my MS thesis. I express my sincere respect and gratitude to my all teachers who have given their valuable support cooperation and suggestion from time to time in my study.
Special thanks to my family. Words cannot express how indebted I am to my mother and her prayers who always remained a source of inspiration and encouragement. I extend my deepest emotions of appreciation, gratitude, moral support, and indebtedness to my colleague Sanaullah Warraich who made it possible for me to be able to complete my MS degree.

Abstract

The goal of this thesis to investigate the consequence of thermal stratification, thermal radiation, heat source/sink, the gyrotactic microbes in the nanofluid is important to enhance the thermal proficiency of various systems like bacteria live micro-mixers, microbial fuel cells, micro volumes such as enzymatic biosensor, microfluid flow devices, and chip shaped microdevices as bio-micro systems. In addition, the motivating research area in the current era is the suspension of nanoparticles with microorganisms which plays a vital role in the field of biotechnology and biomedical implementations. With this motivation, the purpose of this examination is to give an analysis of gyrotactic microbes bioconvection occurrence for the flow of Reiner-Philippoff (R-P) nanofluid in presence of thermal radiation and heat source-sink within a non-uniform thickness over a stretching surface. The governing equations are partial differential equations which are transformed into a coupled system of nonlinear dimensionless equations. The dimensionless equations are then tackled by a numerical technique (shooting method) using computational MATLAB scheme. The influences of the flow parameters on the velocity, mass and heat transfer rates, motile microbe rate of diffusion is analyzed and demonstrated via graphs and tables. Numerical findings concluded that the bioconvection Peclet number and motile microbe increase the motile microorganism's concentration. Furthermore, the thermal radiation increases the temperature.

TABLE OF CONTENTS

LIST OF TABLES

LIST OF FIGURES

LIST OF SYMBOLS

u, v	Velocity component along x, y direction
x	Co-ordinate along the plate
y	Co-ordinate normal to the plate
U_w	Stretching velocity of sheet
U_0	Reference velocity
C	concentration of fluid
Pr	Prandtl number
Ec	Eckert number
Le	Lewis number
Nu	Local Nusselt number
Sc	Bioconvection Schmidt number
Pe	Peclet number
Re_x	Local non-Newtonian Reynolds number
C_{fx}	Local skin friction coefficient
f, g	Dimensionless velocities
q^*	Heat source/sink
N	Microorganism concentration
N_t	Thermophoresis parameter
N_r	Thermal radiation parameter
N_b	Brownian motion
C_p	Specific heat capacity at constant pressure
C_∞	Ambient concentration
S_t	Thermal stratification
S_t^*	Solutal stratification
b, c, d	Constant

A^*, B^*	Heat generation or absorption parameters
k	Thermal conductivity
D_B	Brownian diffusion coefficient
D_n	Diffusivity of microorganisms,
T_∞	Ambient temperature
T	Temperature,
k_0	Absorption coefficient
U_∞	Free stream velocity
bW_c	Cell swimming speed
D_T	Thermophoretic coefficient

GREEK ALPHABET

η	Similarity variable
μ	Dynamics viscosity
μ_0	Dynamics viscosity (very small)
μ_∞	Dynamics viscosity (very large)
ν	Kinematics viscosity
ρ_f	Density of fluid
γ	Bingham number
ψ	Stream function
α	Wall thickness parameter
τ	Shear stress
Ω	Motile microbe parameter
α^*	Thermal conductivity
σ	Stefan–Boltzmann constant
τ^*	Nanofluid heat capacity ratio

SUBSCRIPTS

f	Fluid
0	Condition at surface
w	Condition at wall

∞	Condition at free stream velocity
r	Radiation
t	Thermal
b	Brownian
f	Fluid

CHAPTER 1

INTRODUCTION

This chapter contains a few significant basic definitions as well as some useful flow laws and equations which help to understand the work related in the next chapters. Moreover, few major concepts of solution methods such as shooting technique and Runge-Kutta method are also discussed.

1.1 Basic Definitions

1.1.1 Fluids

A continually deforming substance due to external force or an applied shear stress is called fluid. Fluid is a form of matter which includes gas or liquid. Liquids have definite volume but do not hold a shape. On the other hand, the gases do not own either a definite shape or volume. The fluid is very common in our daily life such as air, water, petrol, nitrogen, honey, methane, and helium. The field of science that deals with the behavior of fluid is called fluid mechanics. It has wide range of applications in biological sciences, environmental sciences, marine sciences, oceanology, engineering, and study of blood flow etcetera.

1.1.2 Real Fluid

Real fluids or viscous fluids are those which have at least some viscosities. The fluid which possesses zero viscosity is termed as ideal fluid, which does not exist. The real fluid can be categorized as

i. Newtonian fluid
ii. Non-Newtonian fluid

i) Newtonian Fluid

When shear stress on a fluid is applied directly proportional to deformation rate or the fluid that obey the Newton's law of viscosity is identified as Newtonian fluid, where Newton's law of viscosity says that applied shear stress is directly and linearly proportional to the velocity gradient. In Newtonian fluid, the viscosity remains fixed, regardless, how much amount of shear applied for a fix temperature.

Mathematically

$$\tau_{yx} = \mu \frac{du}{dy}, \tag{1.1}$$

where τ represents the shear stress applied on the fluid, μ denotes viscosity of fluid, and $\frac{du}{dy}$ shows that the velocity gradient normal to the direction of shear. Water, mineral oil, and gasoline are the representations of Newtonian fluids.

ii) Non-Newtonian Fluid

Many of the fluids exist in nature whose viscosity vary with the variation of the acting shear stress, such type of fluid observed as non-Newtonian fluids. In other words when shear stress is contradicting the relation of directly proportional to the rate deformation is called non-Newtonian fluid.

$$\tau_{yx} \propto \frac{du}{dy}, \tag{1.2}$$

$$\tau_{yx} = k \left(\frac{du}{dy}\right)^n, \tag{1.3}$$

where n is performance index, $n \neq 1$, when $n > 1$ is called pseudo-plastic and $n < 1$ is known as dilatant fluid and k is constant index.

1.1.3 Bioconvection

Bioconvection is the motion of a large number of small organisms in a fluid, especially free swim zooplankton in water. Microorganisms are well known as unicellular organisms. They live universally, as in human and plant bodies. They are considerable thicker than water, due to which microorganisms develop a cause of bioconvection. Bioconvection's physical significance is proficiently assorted in ethanol, biofuels, and a variety of industrial and environmental structures. The functionality of bioconvection is established by an upsurge in the concentration of motile microorganisms.

1.1.4 Stretching Flow

When the sheet is stretched in its own plane velocity comparative from a fixed point to its distance is known as stretching flow. There are different kinds of stretching flow such as linearly and non-linearly stretching flow.

1.1.5 Variable Thickness of Sheet

In this era, the researchers are focusing over a sheet with nonlinear stretching. Many of the physical circumstances happens in which the need of a nonlinear stretching sheet must be critical. The expression for non-linear stretching $U_w = (x + b)^n$ with n variation, and b represents the variable thickness of extending sheet. Particular form of nonlinearly extending sheet with non-uniform thickness is frequently utilized in acoustical components, architecture, nuclear reactor technology, machine design, and naval structure.

1.1.6 Brownian Motion

It is unsystematic movement of microscopic particles adjourned in a liquid or gas, due to collisions with molecules of the neighboring medium. The Brownian motion is demonstrated and discoursed the indication for the movement of molecules provided by an experiment. The Brownian motion was firstly introduced by Robert Brown in 1827.

1.1.7 Thermal Radiation

The process by which energy is emitted by a warmed surface in all ways and moves at the speed of light directly to its point of absorption. There is not any intervening medium required to carry thermal radiations. The thermal radiation performs a vital role in various mechanical, chemical processing, engineering technologies, and climate change. High absorbers are great emitters, objects with maximum absorption will have maximum emission.

Thermal radiation depends on factors given below

- Shape of the body
- Nature of the surface material
- The temperature of the body

1.1.8 Thermal Stratification

Thermal stratification happens while two natures of steam with various temperatures arise into interaction. The difference in temperature causes the colder and heavier water to settle at the bottom, while permitting the lighter and warmer water to float at over the cooler water. The thermal transport phenomenon is considered by thermal radiation. Thermal radiation has energetic role in industries, airplane, gas turbines etc.

1.1.9 Solutal Stratification

Solutal stratification is that which occur due to its concentration difference or the occurrence of different fluids getting diverse densities. Thermal stratification develops due to temperature variations. Double stratification process in fluid gains much interest in heat and mass transport analysis. In fact, inspecting mixed convection flow over a double stratified medium is a significant fluid problem due to the presence of geo-physical flows like in the lakes, rivers, seas, and solar ponds.

1.1.10 Heat Source/Sink

A heat absorption is an inactive heat exchanger that transfers the heat formed by electronics or a mechanical device into a coolant fluid in motion. A heat source is a body that produces or radiates heat.

1.2 Constitutive Equations

1.2.1 Continuity Equation

Continuity equation states that mass is conserved in such a way when fluid is in motion. Conservation of mass is mathematically represented by continuity equation. It describes the mass of any object of body remains same. This law was given by "Antoine Lavoisier" in 1789. Which can be written mathematically as:

$$\frac{\partial \rho}{\partial t} + \nabla.(\rho\, V) = 0\,, \tag{1.4}$$

where the stability is for incompressible fluid as follows:

$$\nabla.\vec{V} = 0, \tag{1.5}$$

where ρ describes density, t for time, velocity field $V = [u(x,y,z), v(x,y,z), w(x,y,z)]$ and ∇ is the divergence parameter.

1.2.2 Momentum Equation

The general law of physics states that the quantity of momentum that describes motion remains unchanged in isolated system of objects or the sum of momentum remains constant. The momentum equation involves that the time rate of momentum changes in each direction be evenly balanced to total of the forces acting in that direction, this observable fact is also called Newton's second law of motion. The incompressible Navier-Stocks equation is derived form of Newton's second law of motion.

Mathematically it can be written as

$$\rho \left(\frac{\partial \vec{V}}{\partial t} + \left(\vec{V}.\nabla\right)\vec{V}\right) = div\,\tau + \rho\, b. \tag{1.6}$$

where ρb represents body force divided by unit mass, τ is the Cauchy stress tenor, and $\vec{V}$ is the velocity vector.

The Cauchy stress tensor τ has the form

$$\tau = -PI + \mu\, A^*. \tag{1.7}$$

In above equation, P and I express the pressure and identity tensor, respectively and A^* is Rivlin Erickson tensor written as

$$A^* = \nabla V + (\nabla V)^T, \tag{1.8}$$

T denotes transpose of matrix. Given below expression is for three-dimensional flow

$$\nabla\, V = \begin{bmatrix} \frac{\partial u}{\partial x} & \frac{\partial u}{\partial y} & \frac{\partial u}{\partial z} \\ \frac{\partial v}{\partial x} & \frac{\partial v}{\partial y} & \frac{\partial v}{\partial z} \\ \frac{\partial w}{\partial x} & \frac{\partial w}{\partial y} & \frac{\partial w}{\partial z} \end{bmatrix}. \tag{1.9}$$

1.2.3 Concentration Equation

$$\frac{\partial C}{\partial t} + \left(\vec{V}.\nabla\right)C = D\,\nabla^2\, C + k_n\, C^n. \tag{1.10}$$

The equation (1.10) is known as concentration equation, C shows the intensity of the species, D is for diffusion coefficient, and k_n is for reaction rate of the nth order homogeneous chemical reaction.

1.2.4 Boundary layer Equation/Flow

The discovery of boundary layer flow has vital role in fluids. This innovation is done in 1904. The influential Navier-stokes equations of Newtonian fluid flow vastly simplified inside the boundary layer have order of significance analysis of results. Certainly, PDE's turn into parabolic. This process massively achieves solution process for equations. The flow is split up into inviscid term which is easy to solve by several methods, and boundary layer

which will be derived easily to tackled by PDE. Incompressible two-dimensional flow of Navier-stoke equations are

$$u\,\frac{\partial u}{\partial x} + v\,\frac{\partial u}{\partial y} = -\frac{1}{\rho}\,\frac{\partial P}{\partial x} + \nu\left(\frac{\partial^2 u}{\partial x^2} + \frac{\partial^2 u}{\partial y^2}\right), \tag{1.11}$$

$$u\,\frac{\partial v}{\partial x} + v\,\frac{\partial v}{\partial y} = -\frac{1}{\rho}\,\frac{\partial P}{\partial y} + \nu\left(\frac{\partial^2 v}{\partial x^2} + \frac{\partial^2 v}{\partial y^2}\right), \tag{1.12}$$

$$\frac{\partial u}{\partial x} + \frac{\partial u}{\partial y} = 0. \tag{1.13}$$

In above mentioned expressions ν is kinematic viscosity, u and v are the velocity components in x, y direction, respectively. The wall is assumed at $y = 0$, using dimensionless parameters

$$\check{x} = \frac{x}{L}\,, \check{y} = \frac{x}{\delta_0}\,, \check{u} = \frac{u}{U}\,, \check{v} = \frac{v}{U}\,\frac{L}{\delta_0}\,, \quad \check{P} = \frac{P}{\rho U^2}\,. \tag{1.14}$$

here the parameter L indicates horizontal length and δ_0 represents boundary layer thickness.

Equations (1.11 - 1.13) in form of non-dimensional parameters are

$$\check{u}\,\frac{\partial \check{u}}{\partial \check{x}} + \check{v}\,\frac{\partial \check{u}}{\partial \check{y}} = -\frac{\partial \check{P}}{\partial \check{x}} + \frac{\nu}{LU}\,\frac{\partial^2 \check{u}}{\partial \check{x}^2} + \frac{\nu}{LU}\left(\frac{L}{\delta_0}\right)^2 \frac{\partial^2 \check{u}}{\partial \check{y}^2}\,, \tag{1.15}$$

$$\check{u}\,\frac{\partial \check{v}}{\partial \check{x}} + \check{v}\,\frac{\partial \check{v}}{\partial \check{y}} = -\left(\frac{L}{\delta_0}\right)^2 \frac{\partial \check{P}}{\partial \check{y}} + \frac{\nu}{LU}\,\frac{\partial^2 \check{v}}{\partial \check{x}^2} + \frac{\nu}{LU}\left(\frac{L}{\delta_0}\right)^2 \frac{\partial^2 \check{v}}{\partial \check{y}^2}\,, \tag{1.16}$$

$$\check{u}\frac{\partial \check{u}}{\partial \check{x}} + \check{v}\,\frac{\partial \check{v}}{\partial \check{y}} = 0, \tag{1.17}$$

where Reynold's number can be written as

$$R = \frac{UL}{\nu}\,. \tag{1.18}$$

In the boundary layer theory, the inertial forces and viscous forces are of the same order

Hence,

$$\frac{\nu}{UL}\left(\frac{L}{\delta_0}\right)^2 = O(1)\,, \tag{1.19}$$

or

$$\delta_0 = O\left(R^{-\frac{1}{2}} L\right). \tag{1.20}$$

Vanishing tilde notation and utilizing above equation we obtain

$$u\,\frac{\partial u}{\partial x} + v\,\frac{\partial u}{\partial y} = -\frac{\partial P}{\partial x} + \frac{1}{R^2}\left(\frac{\partial^2 u}{\partial x^2} + \frac{\partial^2 u}{\partial y^2}\right), \tag{1.21}$$

$$\frac{1}{R}\left(u\,\frac{\partial u}{\partial x} + v\,\frac{\partial u}{\partial y}\right) = -\frac{\partial P}{\partial x} + \frac{1}{R^2}\left(\frac{\partial^2 v}{\partial x^2} + \frac{\partial^2 v}{\partial y^2}\right), \tag{1.22}$$

$$\frac{\partial u}{\partial x} + \frac{\partial v}{\partial y} = 0. \tag{1.23}$$

For $R \to \infty$, it becomes

$$u\,\frac{\partial u}{\partial x} + v\,\frac{\partial u}{\partial y} = -\frac{\partial P}{\partial x} + \frac{\partial^2 u}{\partial y^2}, \tag{1.24}$$

$$-\frac{\partial P}{\partial x} = 0, \tag{1.25}$$

$$\frac{\partial u}{\partial x} + \frac{\partial u}{\partial y} = 0, \tag{1.26}$$

where Eq. (1.25) reveals that pressure is fixed all over the boundary layer. Dimensional form of Eq. (1.21) - (1.23) become

$$u\,\frac{\partial u}{\partial x} + v\,\frac{\partial u}{\partial y} = -\frac{1}{\rho}\frac{\partial P}{\partial x} + \nu\frac{\partial^2 u}{\partial y^2}, \tag{1.27}$$

$$-\frac{1}{\rho}\,\frac{\partial P}{\partial x} = 0, \tag{1.28}$$

$$\frac{\partial u}{\partial x} + \frac{\partial v}{\partial y} = 0. \tag{1.29}$$

1.3 Solution Methodology

Physical and engineering problems are mostly presented by means of differential equations either ordinary DEs or partial DEs. These ordinary/partial DEs are not easy to

solve. By putting similarity suitable transformations, one convert partial DEs into ordinary DEs which can be solved by numerical methods as well as analytical techniques. Mostly problems of phenomena of universe are originally nonlinear thus they are demonstrated by non-linear equations. Science had groomed up, but it is still much difficult to get accurate solutions of non-linear problems in the form of analytical approximation than numerical solution. A numerical method is given below is used to solve the present problem.

1.3.1 Runge- Kutta Method

Various numerical techniques are used for explaining initial value problems in terms of ordinary differential equations. The most effective technique according to get accurate results was established by two German mathematicians C. Runge and W. Kutta. This method is famous as Runge-Kutta method (RK method) and distinguished due to acceptance of Taylor's series. Fourth order RK method is preferably used to find the numerical solution of linear as well as nonlinear ordinary DEs. The standard form of second order initial value problem is written as

$$\frac{d^2y}{d^2x} = f\left(x, y, \frac{dy}{dx}\right), \tag{1.30}$$

having initial conditions

$$y(x_0) = y_0, \quad \frac{dy}{dx}(x_0) = a, \tag{1.31}$$

for solving the above problem directly, we need to transform second order IVP into the system of first order IVP by taking

$$\frac{dy}{dx} = g(x, y, z) = z, \tag{1.32}$$

therefore, we get

$$\frac{dz}{dx} = f(x, y, z), \tag{1.33}$$

then the initial conditions are

$$y(x_0) = y_0, \; z(x_0) = a. \tag{1.34}$$

For above system of first ODEs with initial conditions, the Runge-Kutta (RK) method is given below

$$y_{n+1} = y_n + \frac{1}{6}(p_1 + p_2 + p_3 + p_4), \tag{1.35}$$

and

$$z_{n+1} = z_n + \frac{1}{6}(q_1 + q_2 + q_3 + q_4), \tag{1.36}$$

where

$$p_1 = h\, g\,(x_n,\ y_n,\ z_n\,), \quad q_1 = h\, f\,(x_n,\ y_n,\ z_n\,), \tag{1.37}$$

$$p_2 = h\, g\left(x_n + \frac{h}{2},\ y_n + \frac{p_1}{2},\ z_n + \frac{q_1}{2}\right),\ q_2 = h\, f\left(x_n + \frac{h}{2},\ y_n + \frac{p_1}{2},\ z_n + \frac{q_1}{2}\right), \tag{1.38}$$

$$p_3 = h\, g\left(x_n + \frac{h}{2},\ y_n + \frac{p_2}{2},\ z_n + \frac{q_2}{2}\right),\ q_3 = h\, f\left(x_n + \frac{h}{2},\ y_n + \frac{p_2}{2},\ z_n + \frac{q_2}{2}\right), \tag{1.39}$$

$$p_4 = h\, g\,(x_n + h, y_n + p_3, z_n + q_3), \quad q_4 = h\, f\,(x_n + h, y_n + p_3, z_n + q_3), \tag{1.40}$$

where the step size is defined as

$$h = \frac{x_n - x_0}{n}, \tag{1.41}$$

here n is the number of steps.

1.3.2 Shooting Method

An iterative technique that is used to change the boundary value problems into initial value problems is called shooting method. By assuming the unknown conditions, the method converts the BVP to some IVP. In shooting method, we must find the solution of one ending point of the boundary value problem and "shoot" to the other ending point with the initial value, unless it converges to the other end of boundary condition or current value. The advantage of this initial value problem method is that it takes good speed and adaptability.

$$\frac{d^2y}{d^2x} = f\left(x, y, \frac{dy}{dx}\right), \tag{1.42}$$

with concern boundary conditions

$$y(0) = 0, \quad y(L) = A, \tag{1.43}$$

where f is an arbitrary function where $x = 0$,and $x = L$. The same DE prescribed an initial value problem if given data is described as

$$y\,(0) = 0, \;\; y'(0) = s. \tag{1.44}$$

We convert (1.42) into system of first order DEs for solving boundary value problem as

$$\frac{dy}{dx} = u, \;\; \frac{du}{dx} = f(x, y, u), \tag{1.45}$$

and initial conditions

$$y(0) = 0, \;\; y'(0) = u(0) = s, \tag{1.46}$$

where s represents the missing initial condition, that will be considered as initial value. After that we will find the nearly true value of s therefore the solution of equation (1.45) according to initial conditions of (1.46) satisfied the boundary conditions (1.43). Particularly, if the solution of the initial value problem is represented as $y = (x, s)$ and $u = (x, s)$, after that searching the value of s,

suppose

$$y(L, s) - A = 0 = \phi^*\,(s). \tag{1.47}$$

Now, by the help of Newton's formula which is a strong technique for solving the equations numerically, we will discover the value of s as we are selecting a root of linear algebraic equation (1.44) as

$$s^{n+1} = s^n - \frac{\phi^*(s^n)}{\frac{d\phi^*}{ds}(s^n)}, \tag{1.48}$$

implies that

$$s^{n+1} = s^n - \frac{y(L,s^n)-A}{\frac{dy}{dx}(L,s^n)}, \tag{1.49}$$

Differentiation of y with respect to s, equation (1.45) and (1.46) give

$$\frac{d\acute{Y}}{dx} = \acute{U}, \quad \frac{d\acute{U}}{dx} = \frac{\partial f}{\partial y}\acute{Y} + \frac{\partial f}{\partial u}\acute{U}, \tag{1.50}$$

where

$$\acute{Y} = \frac{\partial y}{\partial s}, \qquad \acute{U} = \frac{\partial u}{\partial s}, \tag{1.51}$$

and resulting initial condition will be

$$\acute{Y}(0) = 0, \ \acute{U}(0) = 1. \tag{1.52}$$

where prime notion does not represent the derivative.

According to boundary conditions (1.43) can get the solution of the equation (1.42) by the following steps.

(i) $s^{(1)}$ denotes initial guess which is chosen for missing initial condition. (1.46)

(ii) According to initial condition (1.46) from $x = 0$ to $x = L$, will be utilized to solve the system of equations (1.45).

(iii) By integrating the system of equations (1.50) based on initial conditions (1.52) from $x = 0$ to $x = L$.

(iv) Putting the value of $y(L, s^{(1)})$ from the step (ii), and $Y(L, s^{(1)})$ obtained by step (iii) into the equations (1.49) as

$$s^{(2)} = s^{(1)} - \frac{\mathrm{y}\left(L, s^{(1)}\right) - A}{\acute{Y}\left(L, s^{(1)}\right)}, \tag{1.53}$$

next guess of missing initial condition is $s^{(2)}$ obtained.

(v) Repetition of these steps (i) to (iv) until the values of s shows the specified degree of accuracy or solution $y\left(L, s^{(2)}\right)$ satisfied the imposed boundary condition Eq. (1.43).

CHAPTER 2

LITERATURE REVIEW

2.1 Overview

In this chapter we discussed the literature study related to heat and mass transfer, Reiner-Philippoff nanofluid, MHD, bioconvection, stratification, and slendering sheet. The fundamental concepts and technique as well as results are also demonstrated.

2.2 Literature Review

Attention of the number of scientists have been attracted to non-Newtonian fluid in the field of engineering for several years because of its applications in several fields of science and technology. The fluid which does not hold the Newton's law of viscosity but varies as shear stress is proportionally to the nonlinear velocity profile is called non-Newtonian fluid. Scientists and engineers usually deal fluids such as oils, water and air known as Newtonian. While in many situations occurs, the supposition of Newtonian action is not valid or more complex and have to deal with non-Newtonian models. such as conditions arise in plastic and chemical processing industry. Non-Newtonian performance is also found in the mining industry, whereas muds, lubrication, biomedical flows, and slurries are often tackled. Non-Newtonian fluid used in our daily life like ketchup, toothpaste, paint, shampoo, mud, fiber technology, greases, lubricants, plastic etc. In a single relation, the behavior of non-Newtonian fluid under the shear is not predicted. Many mathematical models are formed to recognize the behavior of shear stress and shear strain phenomenon under the consideration of non-Newtonian fluids. Several useful models to understand such fluids are the viscoelastic model, Ellis model, Powell-Eyring model, Sisko model, Carreau viscosity model, Cross viscosity model, and R-P model. Nanofluids have a lot of potential uses in technological processes, thermal engineering, plasma physics, and nuclear engineering in this century. Nanofluids, which are different from traditional fluids, have reached a critical stage in research and industry. Due to their attractive strength, thermal

transfer, and features, nanofluids are increasingly being used as thermodynamic fluids. Because of the applications of nanofluids in numerous areas of biotechnology, the flow of gyrotactic microorganisms in nanofluids is receiving a significantly attention from research scholars and scientists in these days. The Reiner-Philippoff model possesses the family of pseudo plastic/shear-thinning fluid. The specified form of non-Newtonian fluid is R-P fluid. It is assumed to determine the non-Newtonian fluid flow through a non-uniform enlarging surface where thickness is not uniform. It is examined the nature of fluid and surface thickness of fluid for three types of fluids either dilatant, pseudo-plastic or viscous, which are meaningfully differentiate the features of flow, also observed the thickness of the surface can be adopted to handle the skin friction and velocity of fluid. The Bingham number found greater than zero for dilatant fluid, less than zero for pseudo-plastic fluid and zero for the viscous according to the rate of skin friction concluded by Ahmed *et al.* [1]. The researchers Kumar *et al.* [2] determined C-C heat flux appearance on R-P fluid over a perpendicular magnetized field. They concluded that comparatively the lessening of heat transformation is additional in pseudo plastic fluid then others, shrinkage of compactness in momentum layer for excessive values of three cases, i.e, Dilatant, Newtonian, and Pseudo-plastic fluids. Sajid *et al.* [3] examined the effect of heat sink/source, nonlinearly thermal radiation, and variation molecular diffusivity on R-P fluid passing through an extending sheet. A decline in the field of shear stress happens on account of access in the Bingham number but perpendicular behavior is observed in the case of fluid variable. The coefficient of skin friction decreases in the case of dilatant fluid but increases in the case of pseudo-plastic fluid. The certain variation in the kind diffusivity parameter affects an augmentation in the mass friction field.

Na [4] explored the R-P boundary layer flow of fluids across the bodies other than a $90°$ wedge. A conventional formulation is under consideration where boundary layer equation for every body shape can be tackled by a finite difference procedure, in the same way the result of the flow over $90°$ wedge is produced the family of parameters. The classical explanation of the edge layer flow on a flat plate is famous as Blasius solutions, which are created due to non-Newtonian fundamental of the fluids. Authors are paying must interest in the boundary layer flow fluids of $90°$ as well as R-P fluid. The flow of a pure non-Newtonian R–P fluid, the occupancy of nanoparticles through a nonlinearly stretching sheet is

numerically calculated by Ahmed [5]. It is recognized that drag coefficient for dilatant is higher than Pseudo-plastic fluids and heat, nano-particles consolidation fluxes on the surface increase with enhancement in R–P fluid parameter. The parallel expression shows the drag friction is a reducing momentum of R–P fluid. The impact of one parameter is extremely insignificant as compared to other, therefore, variation of only 2nd parameter is observed to illustrate the special impact of non-Newtonian fluid. To decrease Nusselt number is observed a reducing act, but the parameter of Brownian motion and thermophoresis are augmented with increasing R-P fluid parameter.

Tahir [6] determine the influence of pseudo-plastic and dilatant of fluid on pressure gradient, velocity, temperature parameter, and bolus velocity. Given research paper is summarized with key determinations by intensifying the value of the R-P fluid variable, the momentum of fluid enhances at the middle of the channel and reduces near the edges of channel. However, the effect of shear stress variable is totally contradicted on dilatants fluid by comparing with Pseudo-plastic fluid parameter. The value of pressure over pseudo-plastic fluid enhanced as shear stress variable increased. It is noted that hotness of pseudo-plastic fluid improves with an enhancement in shear stress variable. The performance of temperature is contradicted for dilatants fluid to pseudoplastic fluid. Reddy *et al.* [7] focused in their research work is to examine a linear stretching surface and Darcy–Forchheimer medium. There is the capability of developing microorganisms along nanofluids in numerous bio-micro systems, i.e. the reformation of carbohydrates and to estimate harmfulness of nanoparticles in micro-process microprocessor devices by Khan *et al.* [8]. The improved relation for heat and mass transference enquiry encountered considering the theory of C-C heat flux model by Li *et al.* [9]. The author concluded; an increment of R-P fluid is observed to increasing nanofluid velocity as well as microorganism profile. However, velocity profile is reduced by the bouncy force and slip factor. The classical R-P fluid is taken to inspect the flow of non-Newtonian fluid on a non-linearly spreading sheet having non-uniform thickness including the occurrence of thermal radiation and bioconvection is studied. Due to thermal radiation influence the heat transfer rate decreases while the energy increases. Peclet number and Schmidt number of bioconvection is tend to drop the density profile and improve the diffusion rate of microorganism summarized by Ahmed *et al.* [10]. The consequence of bioconvection microorganism in (Buongiorno) nanofluid flow by stretching sheet

considering MHD, chemically reactant, Brownian motion, activation energy, and thermophoresis diffusion. The concentration profile enhances the temperature and activation energy is observed to enhance the thermophoresis as well as Brownian parameter by Chu *et al.* [11]. The magnetic flow through a R–P nanofluid and heat transfer augmentation on the extending surface under the impression of solar radiation is examined by Reddy *et al.* [12]. The work is finished by concluding, generation and transformation of heat is spread in non-uniform radiation as compere to linear radiation, the influence of Pseudo-plastic, dilatant, and Newtonian fluid are highly differentiation in higher values of Hartman number. Effect of pseudo-plasticity and dilatancy of liquid on peristaltic flow and heat transformation is scrutinized described Tahir and Ahmad [6]. The research paper is summarized with key observation which is by growing the value of R-P fluid parameter the velocity of fluid increases at the middle of the channel and drops close the boundary of the channel.

The impact of thermal stratification is an essential phase in mass and heat transfer. Fluid stratification is observed due to change in temperature, the difference of concentration, or the occurrence of distinct fluids of various thicknesses. In the specific condition where mass and heat transfer are considered instantaneously, it is essential to examine the influence of dual stratification upon the convective transportation in nanofluids. Thermally stratified fluids can be found in practically every heterogeneous fluid body in nature. The density variations have a major influence on the dynamics and combining of heterogeneous fluids in the presence of gravity. Thermal stratification in reservoirs, for example, it can decrease vertical oxygen combination to the point that underneath water be converted into anoxic due to biological processes. However, conditional on other limnological mixed layer factors, understanding the dynamic contrast of stratified fluids is required for avoiding, predicting, and fixing such a reservoir difficulty. In lakes and ponds, the concept of stratification is crucial. Controlling temperature stratification and hydrogen and oxygen concentration differences in such conditions is critical because they may have a direct impact on the growth rate of all kinds of species. Thermal stratification analysis is also significant for solar engineering since better stratification can be observed in improved energy proficiency [13-16].

Rehman *et al.* [17]. observed the occurrence of mixed convection consequence both the fluid concentration and temperature are declining parameters of solutal stratification

along with thermal stratification respectively. They found values are qualified by improving assessment with present values and an outstanding settlement is witnessed which approves the performance of computational software. The temperature and concentration profile are noted declining by thermal and solutal stratification respectively. The thickness of the velocity boundary layer decline with an upsurge thermal and solutal stratification. The temperature profile is decrease with an augmentation of the values of S_t. The solutal stratification is boosting up by Sherwood number and local Nusselt number described by Ibrahim and Makinde [18]. Thermal stratification in partially ionized hybrid nano-fluid flow on non-linear extended sheet has been discoursed by Chung *et al.* [19].which declare the final remarks, the surface skin coefficient and the rate of heat flux show increasing and decreasing respectively for the augmentation of the S_t parameter.

Shah *et al.* [20] summarized that the thin film thickness of nanofluid decreases with improved magnetic parameter. The nano-fluid temperature was increased with improving value of thermal radiation. The temperature flow to increase due to increment the thermal radiation parameter. And temperature profile reduced when Prandtl number increases. The encouragement of gold nanoparticle with the oxytactic microorganism on radiative R-P fluid due to stretchable sheet. The process of motile density and heat transfer profile with an intensification in Peclet number is investigated is investigate. The density of microorganism profile run down on the behalf of an enlargement in Peclet number by Sajid *et al.* [21]. Cross diffusion properties on magnetic and multiple slip flow of Carreau liquid on a slendering sheet in the existence of non-linear heat generation and absorption is presented by Raju *et al.* [22]. It is resolved, the temperature is a growing function of heat source/sink parameter. Multiple slip apparatus has a trend to increase the velocity profile and declines the temperature fields. Whereas the space and temperature dependent heat sink are desirable for actual cooling of the extending sheet. The outcome of chemical reaction and Brownian motion on the concentration are scrutinized by Qayyum *et al.* [23]. heat generation or absorption and nonlinear convection is under consideration. The non-linear moveable sheet with convectively heated is taken out. The Brownian motion is improved when the concentration of nano particles declined. Thermally analysis in non-steady radiative Maxwell nanofluid flow subject to heat generation/absorption is considered by Ahmed *et al*. [24]. They detected that the thermophoresis factors and Brownian motion augment the thermal

energy transfer in nanofluid flow. Influence of temperature supported heat source or sink and non-uniform species diffusivity on R–P radiative fluid is investigated by Sajid *et al.* [25, 26]. They concluded that a certain difference in the Pe directs to a decline in the solute element. The result exposed that certain variation the heat generation/absorption parameter produces more heat to yields and improvement the temperature field.

Magnetic flow of Powell-Eyring nanofluid utilizing variable thickness on a non-uniform extending sheet is analyzed by Hayat *et al.* [27]. It is decided that qualitative performances of temperature and thickness of thermal layer are comparable for radiation as well as temperature ratio parameters. Increment the wall thickness parameter is witnessed to decreases the velocity and temperature profiles. Hayat *et al.* [28, 29] calculated the fluid flow and heat transfer of thixotropic and walters-B nanoliquid. An augmentation in heat generation/absorption display rise to temperature profile. Thermal profile and heat transfer enhance the temperature ratio parameter outcome of thermophoresis parameter and Brownian motion are pretty opposite for concentration field. Flow of nano-liquid with non-uniform stretching and porous velocities over a extending sheet with non-uniform thickness is investigated by Alam *et al.* [30]. The investigation for the boundary layer quiescent fluid over the permeable stretched flat surface is presented by Cortell Rafeal [31]. MHD and effects of viscous dissipation on nonlinear shrinking sheet using R-P fluid model is analyzed by Kashi'ie *et al.* [32]. They concluded that the impact of suction has a remarkable increment on the flow of R-P fluid by enhancing the suction parameter. The entropy improved Darcy-Forchheimer flow of R-P fluid along with chemical reaction is modeled by Xiong *et al.* [33]. Bioconvective flow of nanofluid inclosing gyrotactic motile microbes over a non-uniform extending surface is analyzed by Mondal and Pal [34]. Hatami and Jing [35].

It is detected from the studies described above that no such work is done in which the Reiner-Philippoff gyrotactic microorganism nano-fluid flow on a slendering sheet with thermal stratification under the impact of non-linear heat source/sink. The collective study of thermal stratification, thermal radiation, heat source-sink, the gyrotactic microorganisms in nanofluids is important to augment the thermal proficiency of various systems like bacteria live micro-mixers, microbial fuel cells, micro volumes such as enzymatic biosensor, microfluid flow devices, and chip shaped microdevices as bio-micro systems. In addition, the motivating research area in the current era is the suspension of nanoparticles with

microorganisms which plays a vital role in the area of biotechnology and biomedical implementations. With this motivation, the purpose of this examination is to give an analysis of gyrotactic microbes bioconvection occurrence for the flow of Reiner-Philippoff (R-P) nanofluid in attendance of radiation and heat source/sink within a non-uniform thickness over a spreading surface. The inspirations of numerous physical governing aspects on velocity, concentration profiles, temperature, concentration of microorganisms with drag friction coefficient, Sherwood number, Nusselt number, and density number of motile microbes (local) are analyzed numerically and shown via tabular and graphical illustrations.

CHAPTER 3

REINER-PHILIPPOFF FLUID FLOW PASSING THROUGH A STRETCHING SHEET WITH VARIABLE THICKNESS

3.1 Introduction

This section consists characteristics of the R-P fluid across a non-uniform stretching sheet having variable thickness. The solution of considered boundary layer equation is carried out and determined the effect of non-uniform enlarging sheet in the existence of variable thickness of wall considering the flow of R-P fluid. The mathematical model is formulated in PDE's formed. The governing equation are converted into system of non-linear first order ODE and solved be the numerical technique. The obtained results are discussed in detail and presented graphically. This chapter contains review of research done by Ahmed *et al.* [1].

3.2 Mathematical Formulation

Consider 2-dimensional, laminar, incompressible, and steady-state flow of R-P fluid through a continuously stretched sheet and non-uniform wall thickness. It is assumed that $x-$axis along the plane of the extendable sheet and $y-$axis is the perpendicular to the sheet. The sheet consists of non-uniform variable width with given profile $y = A\ (x + b)^{1/3}$. The velocity of the flow is determined by the stretching sheet of the form $U_0(x + b)^{1/3}$. Figure 3.1 is based on boundary layer assumptions. The correlation among shear stress τ and shear strain $\frac{\partial u}{\partial y}$ of R-P fluid is written as [1]:

$$\frac{\partial u}{\partial y} = \frac{\tau}{\mu_\infty + \frac{\mu_0 - \mu_\infty}{1+(\tau/\tau_S)}}$$

for R-P fluid model. The governing equations are mentioned blow:

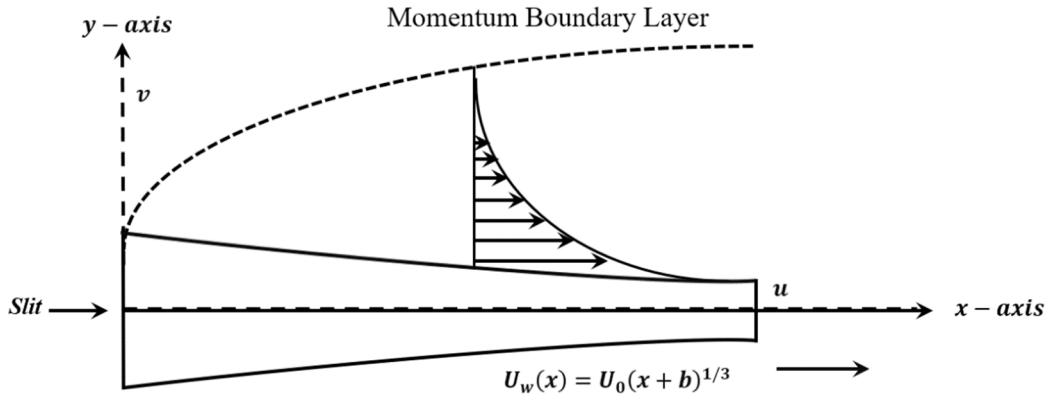

Figure 3.1: Physical configuration of the problem

$$\frac{\partial u}{\partial x} + \frac{\partial v}{\partial y} = 0, \tag{3.1}$$

$$u\frac{\partial u}{\partial x} + v\frac{\partial u}{\partial y} = \frac{1}{\rho_f}\frac{\partial \tau}{\partial y}. \tag{3.2}$$

The suitable boundary conditions are

$$\left.\begin{aligned} u(x,y) = U_w(x) = U_0(x+b)^{\frac{1}{3}} \\ v(x,y) = 0, \end{aligned}\right\} \quad \text{at} \quad y = A(x+b)^{\frac{1}{3}}, \tag{3.3}$$

$$u(x,y) \to 0 \quad \text{as} \quad y \to \infty. \tag{3.4}$$

The solution of the above equation is obtained through given similarity transformations

$$\eta = \sqrt{\frac{U(x)}{\nu}}\, y, \quad \psi = \sqrt{U(x)\, x\, \nu} f(\eta), \quad \tau = \rho\sqrt{U_0^3\, \nu} g(\eta)\,, \tag{3.5}$$

The transformed equations (3.1) and (3.2) into ordinary DEs are given below

$$g' = \frac{1}{3} f'^2 - \frac{2}{3} f f'', \tag{3.6}$$

$$g = f''\left(\frac{g^2 + \lambda \gamma^2}{g + \gamma^2}\right). \tag{3.7}$$

and correspond boundary conditions are

$$f'(\alpha) = 1,\ f(\alpha) = \frac{\alpha}{2} \quad \text{at} \quad \eta = \alpha,\ f' \to 0 \ \text{as} \ \eta \to \infty. \tag{3.8}$$

where Reiner-Philippoff fluid parameters are $\lambda(=\mu_0/\mu_\infty)$ and $\gamma = \left(\tau_s/\rho\sqrt{U_0^3\,\nu}\right)$. The value $\lambda = 1$ is for viscous fluid, $\lambda < 1$ shows the performance of dilatant fluid and $\lambda > 1$ corresponds the behavior of pseudo-plastic. The rate of the yield stress to viscous stress given by γ parameter which is Bingham number.

Now defining $F(\xi) = F(\eta-\alpha) = f(\eta)$ and $G(\xi) = G(\eta-\alpha) = g(\eta)$ the boundary value problem (3.5)-(3.7) result the given form

$$G' = \frac{1}{3}F'^2 - \frac{2}{3}F\,F'', \tag{3.9}$$

$$G = F\,\frac{G^2+\lambda\gamma^2}{G^2+\gamma^2}. \tag{3.10}$$

According to given boundary conditions

$$F'(\xi) = 1,\ \ F(\xi) = \frac{\alpha}{2} \quad \text{at} \quad \xi = 0,\ \ F \to 0 \quad \text{as} \quad \xi \to \infty. \tag{3.11}$$

The skin friction is given as

$$C_{fx} = \frac{\tau}{\frac{1}{2}U_w}, \tag{3.12}$$

The dimensionless form of skin friction converted as

$$\frac{1}{2}C_{fx}\,Re_x^{1/2} = g(0). \tag{3.13}$$

3.3 Solution Methodology

The solution of nonlinear boundary layer problem (3.9) – (3.10) is to be tackled by utilizing the numerical technique, known as shooting technique.

$$\left.\begin{aligned} y_1' &= y_2 y_1(0) = 0, \\ y_2' &= \frac{y_3(y_3^2+\gamma^2)}{(y_3^2+\lambda\gamma^2)}, \qquad y_2(0) = 1, \\ y_3^2 &= \frac{1}{3}y_2^2 - \frac{2}{3}y_1 y_2', \qquad y_3(0) = s. \end{aligned}\right\} \tag{3.14}$$

with corresponding boundary conditions:

$$y_1 = 0, \quad y_2 = 1 \text{ at } \quad \eta = 0, \tag{3.15}$$

$$y_2 = 1 \quad \text{as} \quad \xi \to \infty. \tag{3.16}$$

The resulting momentum equations (3.9)-(3.10) with correspond initial conditions can be tackled using IVP solving technique that is Runge-Kutta technique, by using f as a known function indicating $f = y_1$, $f' = y_2$, g by the y_3 and the absent initial condition by s, the momentum equations of (3.9) and (3.10) are transformed into system of first order ODE's (3.14).

3.4 Results and Discussion

Shooting technique and RK method are used for solving nonlinear ODEs numerically. By the above-mentioned method, the physical parameters are analyzed in this section. It is determined that the consequence of wall thickness variable α over the velocity variation in figure 3.2. We have seen that velocity is gradually declining with growing of α. In physical aspect, with the wall thickness variable, the stretching velocity decreased which decreased the velocity of the fluid flow in boundary. In the numerical solution we must obtained dual solution using the initial estimates of the missing value and in which all the velocity satisfies boundary conditions on infinity according to the thickness of boundary layer with parameter values. Repeat the initial guess up to the precision iteration method. To compare the current numerical outcome is given to demonstrate the sustainability and precision of the current technique and this is obtained a good argument. In figure 3.3 we observed the boundary layer thickness and velocity increase with inclining values of λ and the derivative of the velocity decreased as λ rises, i.e. the phenomena of fluid dilatant, viscous, and pseudo-plastic. In figure (3.4-3.6), the coefficient of drag friction is plotted individually for dilatant, Newtonian, and pseudo-plastic fluids for varying thickness parameters and Bingham number. As physically expected, wall thickness has declining impact of drag friction irrespective of the nature of fluid, having fixed thickness of the surface. We concluded the fluid obey the Reiner-Philippoff model, the magnitude of the friction is observed by the pseudo-plastic fluid when the sheet is enhanced than viscous fluid, and magnitude of the friction of dilatant fluid is less than the viscous fluid. In figure 3.4, it is shows that the skin is decreasing by inclining the parameter of Rainer-Philipoff fluid γ for

the dilatant case, because of the dilatant fluid appeared viscosity increases by inclining the shear rate. The same movement is opposed for the pseudo-plastic fluid, i.e. The dynamic viscosity remains fixed, $\lambda = 1$ at high and at low shear rate, it becomes independent system of parameter γ and therefore, the skin coefficient remains same with λ. It is observed that the ratio of yield stress to the viscous stress which is Bingham number denoted as γ, it rises in the case of skin friction for dilatant fluid. It is noted constant behavior for the viscous fluid and decreasing behavior for the pseudo-plastic fluid. Moreover, the non-Newtonian fluid in figure 3.4-3.6 shows that when yield stress is less than viscous stress ($\lambda < 1$) the difference in skin friction is higher as compared to system where the yield stress overlooks the viscous stress ($\lambda > 1$).

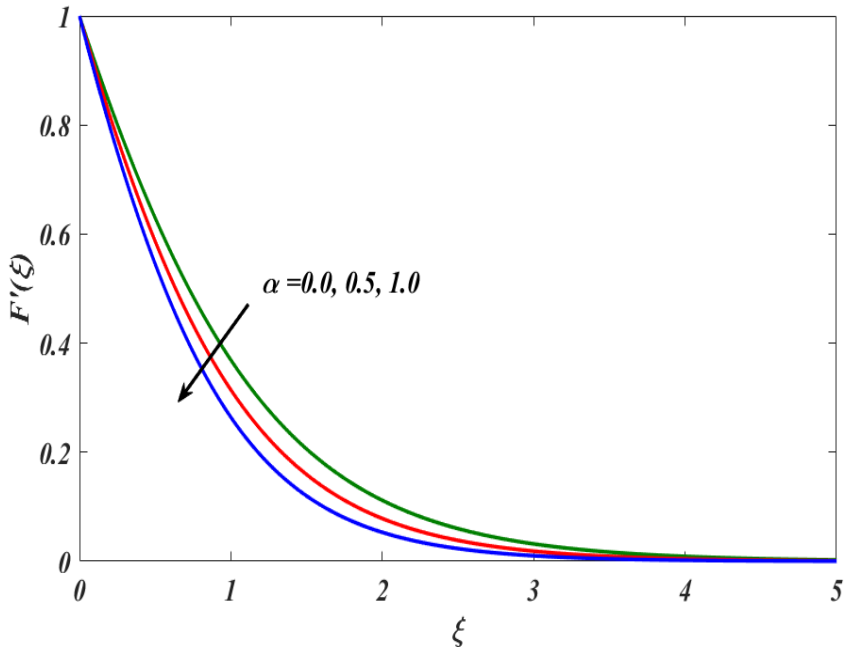

Figure 3.2: Velocity parameter for variation of surface thickness α with $= 1$, $\lambda = 0.5$.

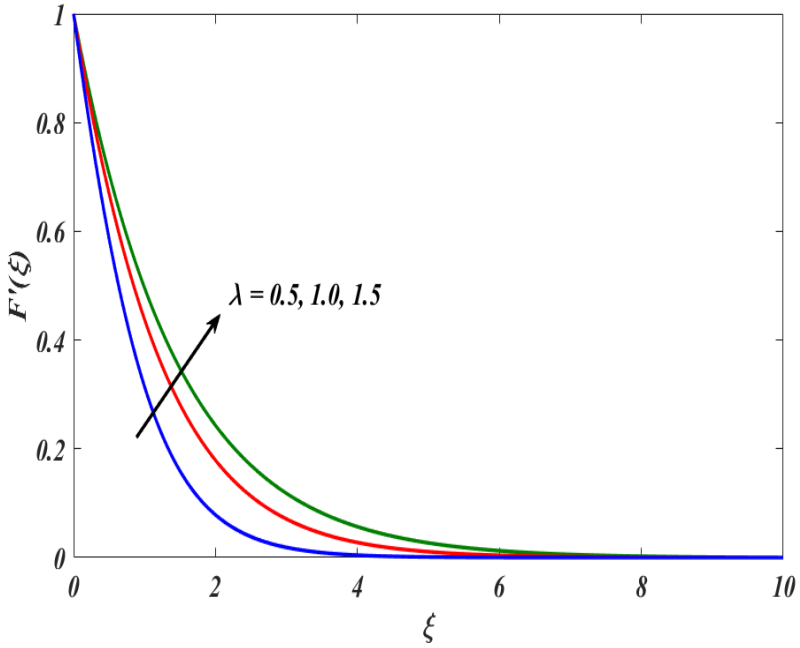

Figure 3.3: Velocity parameter for varying λ with $\alpha = 0.5$ and $\gamma = 1.0$.

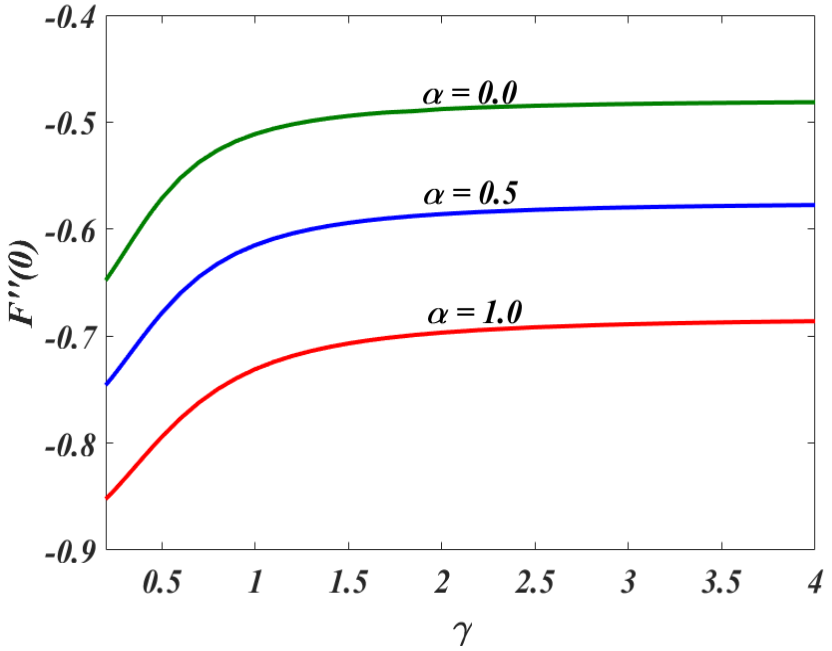

Figure 3.4: Dilatant fluid (skin friction varying concerned parameters, where $\lambda = 0.5$).

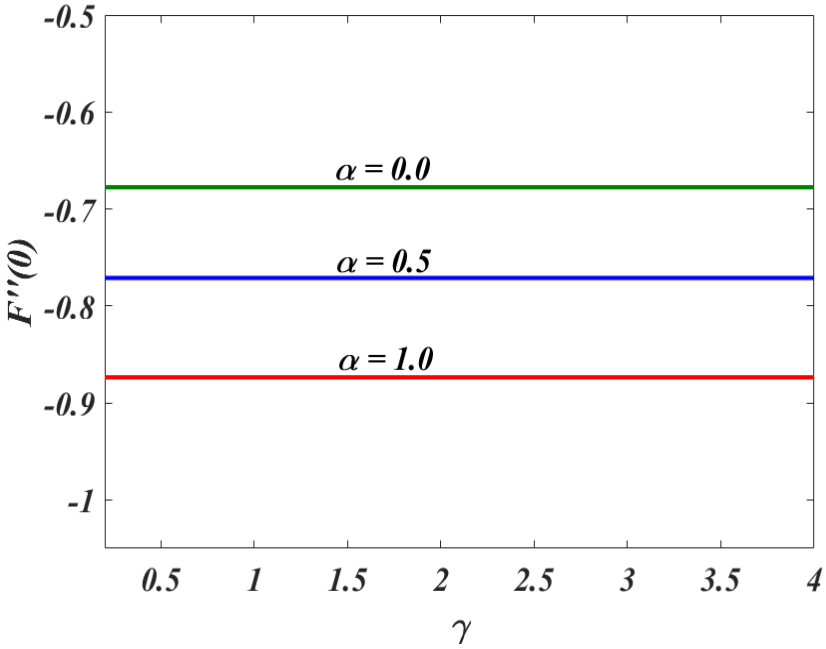

Figure 3.5: Viscous fluid (skin friction varying involved parameters, where $\lambda = 1.0$).

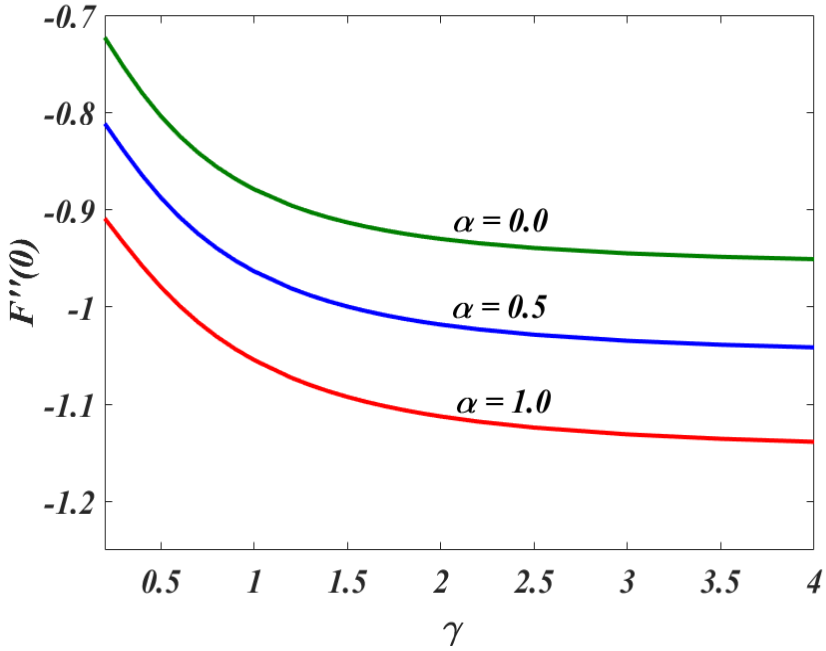

Figure 3.6: Psuedo-plastic fluid (skin friction coefficient variation of involved parameters, where $\lambda = 2.0$.

CHAPTER 4

EFFECT OF DOUBLE STRATIFICATION AND HEAT SOURCE/SINK ON BIOCONVECTION IN REINER-PHILIPPOFF BASED NANOFLUID FLOW THROUGH SLENDERING SHEET

4.1 Overview

The major object of this chapter is to explore the impression of the Reiner-Philippoff gyrotactic microorganism nanofluid flow on a slendering sheet through thermal stratification having non-linear heat source or sink. With the help of similarity transformations, partial DEs are modified into dimensionless ordinary DEs. By using shooting technique, the numerical results are obtained along with R-K method. The impacts of several existing governing factors on velocity, concentration profiles, temperature, and concentration of microorganisms with drag friction coefficient, local Nusselt number, local Sherwood number, local density number of motile microbes are analyzed, and numerical results are interrogated and displayed via tables and graphs.

4.2 Description of Problem

A two-dimensional steady flow of nanofluids including both gyrotactic microbes and nanoparticles across a sheet with non-linear thickness is assumed under the impact of thermal radiation and double stratification. It is assumed that $x-$axis is along the plane of the spreading surface and $y-$axis is normal to the sheet. The fluid temperature, nanofluid concentration, and concentration of the microorganisms over the nonlinearly stretchable surface are denoted by T_w and C_w and N_w. The width of the sheet is considered non-uniform having variable profile $y = A(x + b)^{1/3}$. The velocity of extending sheet is signified as $U_w = (x + b)^{1/3}$. No change is seen in the occurrence of nanoparticles for the swimming pathway of microorganisms and their velocities. But microbe movement is

involved if the volume fraction of nanoparticles is bigger than 1%. Therefore, the mandatory bioconvection permanence is accomplished by the combination of microbes and dense nanoparticles in base fluid. Momentum, thermal, and species boundary layers inside flow treatment are demonstrated in Figure 4.1. The connection between shear stress τ and shear strain $\frac{\partial u}{\partial y}$ is written as [1].

$$\frac{\partial u}{\partial y} = \frac{\tau}{\mu_\infty + \frac{\mu_0 - \mu_\infty}{1 + (\tau/\tau_s)}}.$$

Here, τ_s is the reference shear stress of the non-Newtonian R–P fluid model, μ_0 and μ_∞ represent the dynamics viscosities at very small and extremely large values respectively.

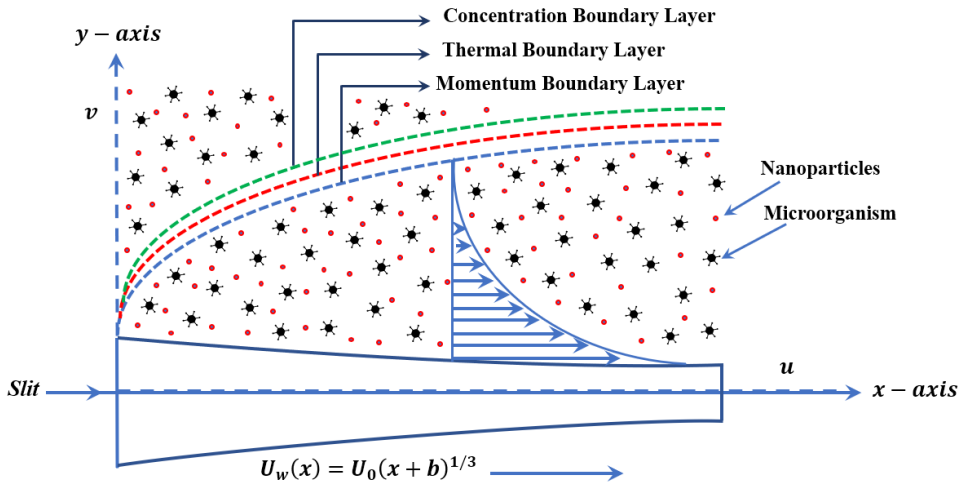

Figure 4.1. Flow Configuration

The flow model of governing equations, in the presence of linear thermal radiation, thermal stratification and source/sink, can be stated as[10, 36]:

$$\frac{\partial u}{\partial x} + \frac{\partial v}{\partial y} = 0, \tag{4.1}$$

$$u\frac{\partial u}{\partial x} + v\frac{\partial u}{\partial y} = \frac{1}{\rho_f}\frac{\partial \tau}{\partial y}, \tag{4.2}$$

$$u\frac{\partial T}{\partial x} + v\frac{\partial T}{\partial y} = \tau\frac{D_T}{T_\infty}\left(\frac{\partial T}{\partial y}\right)^2 + \alpha^*\frac{\partial^2 T}{\partial y^2} + \frac{16\,\sigma\,T^3}{3\,k_0\,\rho C_p}\frac{\partial^2 T}{\partial y^2} + \tau^* D_B\frac{\partial C}{\partial y}\frac{\partial T}{\partial y} + \frac{q^*}{\rho C_p}, \tag{4.3}$$

$$u\frac{\partial C}{\partial x} + v\frac{\partial C}{\partial y} = D_B\frac{\partial^2 C}{\partial y^2} + \frac{D_T}{T_\infty}\frac{\partial^2 T}{\partial y^2}, \tag{4.4}$$

$$u\frac{\partial N}{\partial x} + v\frac{\partial N}{\partial y} + \frac{b\,W_c}{(C_w - C_0)}\frac{\partial}{\partial y}\left[N\left(\frac{\partial C}{\partial y}\right)\right] = D_n\frac{\partial^2 N}{\partial y^2}, \tag{4.5}$$

Boundary conditions are given below

$$\left.\begin{aligned} u(x,y) = U_w(x) = U_0(x+b)^{\frac{1}{3}}, \quad v(x,y) = 0, \\ T = T_w = T_0 + c(x+b)^{\frac{1}{3}}, \\ C = C_w = C_0 + c^*(x+b)^{1/3}, \quad N = N_w, \end{aligned}\right\} \text{at } y = A(x+b)^{1/3},$$

$$\left.\begin{aligned} u(x,y) \to 0, \\ T \to T_\infty = T_0 + d(x+b)^{\frac{1}{3}}, \\ C \to C_\infty = C_0 + d^*(x+b)^{1/3}, \quad N \to N_\infty, \end{aligned}\right\} \text{as } y \to \infty. \tag{4.6}$$

The non-linear heat source/sink parameter q^* is identified as [22]

$$q^* = \frac{kU_w}{\nu(x+b)}\left(\frac{A^*(T_w - T_0)}{U_0(x+b)^{\frac{1}{3}}}u + B^*(T - T_\infty)\right).$$

Here $A^*, B^* > 0$ communicates to interior heat generation and $A^*, B^* < 0$, relates to heat absorption constants respectively.

The dimensionless coordinates used [10] are given below to modify the relevant PDEs (4.1)–(4.5) into ODEs:

$$\eta = \sqrt{\frac{d}{\nu}}\frac{y}{(x+b)^{\frac{1}{3}}}, u = U_0(x+b)^{\frac{1}{3}}f', v = \frac{d\,yf'}{3(x+b)^{\frac{2}{3}}} - \frac{2}{3}\frac{\sqrt{d\,\nu}\,f}{(x+b)^{\frac{1}{3}}},$$

$$\tau = \rho_f\sqrt{U_0^3\nu}\,g(\eta)$$

$$\Theta(\eta) = \frac{T - T_{\infty,0}}{T_w - T_{\infty,0}} - \frac{d(x+b)^{\frac{1}{3}}}{T_w - T_{\infty,0}}, \qquad \varphi(\eta) = \frac{C - C_{\infty,0}}{C_w - C_{\infty,0}} - \frac{d^*(x+b)^{\frac{1}{3}}}{C_w - C_{\infty,0}},$$

$$h(\eta) = \frac{N - N_\infty}{N_w - N_0}.$$

Using similarity transformations in equations (4.2-4.5), we attain the given dimensionless equations:

$$g = f'' \frac{g^2 + \lambda\gamma^2}{g^2 + \gamma^2}, \tag{4.7}$$

$$g' = \frac{1}{3} f'^2 - \frac{2}{3} f f'', \tag{4.8}$$

$$\Theta''\left(\frac{1}{Pr} + \frac{4}{3}Nr\right) + \frac{2}{3} f \Theta' - \frac{f'}{3} S_t + N_t \Theta'^2 + N_b \Theta'\varphi' + \frac{1}{Pr}(A^* f' + B^*\Theta) = 0, \tag{4.9}$$

$$\frac{1}{Sc}\left(\varphi'' + \frac{N_t}{N_B}\Theta''\right) + \frac{2}{3} f\varphi' - \frac{f'}{3} S_t^* = 0, \tag{4.10}$$

$$h'' = Pe(h\varphi'' + \varphi' h + \Omega\,\varphi'') - \frac{2}{3} Lefh', \tag{4.11}$$

Associated boundary conditions take the form

$$\left.\begin{gathered} f'(\alpha) = 1,\ f(\alpha) = \frac{\alpha}{2},\ \Theta(\alpha) = 1 - S_t,\ \varphi(\alpha) = 1 - S_t^*,\ \ h(\alpha) = 1 \ \text{ at } \ \eta = \alpha \\ f' \to 0,\ \Theta \to 0,\ \ \varphi \to 0,\ h \to 0 \quad \text{as} \quad \eta \to \infty. \end{gathered}\right\}, \tag{4.12}$$

By following Hayat *et al.* [37], we convert the domain $[\alpha, \infty]$ into $[0, \infty]$ by utilizing the following strategy.

$$f(\eta) = F(\eta - \alpha) = F(\xi),\ g(\eta) = G(\eta - \alpha) = G(\xi),\ \Theta(\eta) = \theta(\eta - \alpha) = \theta(\xi),$$

$$\varphi(\eta) = \phi(\eta - \alpha) = \phi(\xi), h(\eta) = H(\eta - \alpha) = H(\xi).$$

We get,

$$G' = \frac{1}{3} F'^2 - \frac{2}{3} FF'', \tag{4.13}$$

$$\theta''\left(\frac{1}{Pr}+\frac{4}{3}Nr\right)+\frac{2}{3}\,F\,\theta'-\frac{F'}{3}S_t+N_t\,\theta'^2+N_b\,\theta'\phi'+\frac{1}{Pr}(A^*F'+B^*\theta)=0, \qquad (4.14)$$

$$\frac{1}{Sc}\left(\phi''+\frac{N_t}{N_B}\theta''\right)+\frac{2}{3}F\phi'-\frac{F'}{3}S_t^*=0, \qquad (4.15)$$

$$H''=Pe(H\phi''+\phi'H+\Omega\,\phi'')-\frac{2}{3}\,Le\,FH', \qquad (4.16)$$

with boundary conditions

$$F'(\xi)=1,\ F(\xi)=\frac{\alpha}{2},\ \theta(\xi)=1-S_t,\ \phi(\xi)=1-S_t^*,H(\xi)=1,\quad \text{at}\quad \xi=0,$$

$$F'\to 0,\ \theta\to 0,\ \phi\to 0,\ H\to 0,\ \text{as}\ \xi\to\infty, \qquad (4.17)$$

where α represents the wall thickness, $S_t=\frac{d}{c}$, and $S_t^*=\frac{d^*}{c^*}$ denote thermal and solutal stratification parameters for temperature and concentration respectively. R-P fluid parameter (λ), Bingham number (γ), Peclet number (Pe), Prandtl number (Pr), thermal diffusivity (α^*) bio-convection Lewis number (Le), motile microbe parameter (Ω), thermophoresis parameter(N_t), thermal radiation parameter (N_r), Brownian motion N_b, are mathematically expressed as

$$\lambda=\left(\frac{\mu_0}{\mu_\infty}\right),\qquad \gamma=\left(\frac{\tau_s}{\rho}\sqrt{U_0^3\,\nu}\right),\qquad Pe=\frac{bW_c}{D_n},\qquad Pr=\frac{\nu}{\alpha^*},\qquad \alpha^*=\frac{k}{\rho C_p},\qquad Le=\frac{\nu}{D_n},$$

$$\Omega=\frac{N_{\infty,0}}{N_w-N_{\infty,0}},\ N_t=\frac{\tau^*D_T}{\nu\,T_\infty}\left(T_w-T_{\infty,0}\right),\ \ N_r=\frac{4\sigma\,T_\infty^3}{k_0\mu C_p},\ \ N_b=\frac{\tau^*D_B}{\nu}\left(C_w-C_{\infty,0}\right).$$

The primary important physical quantities such as skin friction coefficient, Nusselt number, local Sherwood number and local density of motile microbe in dimensionless form can be expressed as:

$$-C_{fx}=Re_x^{-\frac{1}{2}}G(0),\quad -Nu_x=Re_x^{\frac{1}{2}}\left(1+\frac{4}{3}N_r\right)\theta'(0),\quad -Sh_x=Re_x^{\frac{1}{2}}\phi'(0),$$

$$-Nn_x=Re_x^{\frac{1}{2}}H'(0).$$

4.3 Solution Methodology

There are several ways to obtain solution of non-linear differential equation. but due to accuracy it is considered an approximate solution of flow equations, a numerical approach is used. The shooting scheme and RK method are often used to follow the numerical treatment with the support of the MATLAB computational program. The numerical method RK method is famous due to its accuracy.

The mentioned approximation is recommended to start the technique assuming $y_1 = F, y_2 = F', y_3 = G, y_4 = \theta, y_5 = \theta', y_6 = \phi, y_7 = \phi', y_8 = H, y_9 = H'$.

$y_1' = y_2,$ $y_2' = \frac{y_3(y_3^2 - \gamma^2)}{y_3^2 + \lambda\gamma^2},$ $y_3' = \frac{1}{3}y_2^2 - \frac{2}{3}y_1 y_2',$ $y_4' = y_5,$ $y_5' = \frac{\frac{y_2}{3}S_t - \frac{2}{3}y_1 y_5 - N_t y_5^2 - N_b y_5 y_7 - \frac{1}{Pr}(A^* y_2 + B^* y_4)}{\left(\frac{1}{Pr} + \frac{4}{3}N_r\right)},$ $y_6' = y_7,$ $y_7' = \frac{y_2}{3}S_t^* - \frac{2}{3}Sc\, y_1 y_7 - \frac{N_t}{N_b}y_5',$ $y_8' = y_9,$ $y_9' = Pe\, y_7'(y_8 + \Omega) + Pe\, y_7 y_8 - \frac{2}{3}Le y_1 y_9,$	$y_1(0) = \frac{\alpha}{2}$ $y_2(0) = 1$ $y_3(0) = u(1)$ $y_4(0) = 1 - S_t$ $y_5(0) = u(2)$ $y_6(0) = 1 - S_t^*$ $y_7(0) = u(3)$ $y_8(0) = 1$ $y_9(0) = u(4)$
$y_2 \to 0, \quad y_4 \to 0, \quad y_6 \to 0, \quad y_8 \to 0,$ as $\xi \to \infty.$	

4.4 Results and Discussions

The governing dimensionless and highly non-linear ODEs (4.14–4.16) are solved using the RK method by using MATLAB. The velocity $F(\xi)$, temperature $\theta(\xi)$, concentration $\phi(\xi)$, and motile microbes density distribution $H(\xi)$ appear asymptotic in behavior for the preferred values of ξ. Three types of fluid are discussed i.e. $\lambda < 1$, $\lambda = 1$, and $\lambda > 1$ for Dilatant, Newtonian, and pseudo-plastic fluid respectively. The behaviours of all three kinds are discussed under the impression of different physical constraints while the rest of the parameters remain constant as $N_t = N_b = N_r = Pe = Le = 0.4$, $\gamma = 0.5$, $\alpha = Pr = Sc = 1$, $A^* = B^* = -0.2$, $S_t = S_t^* = 0.1$, $\Omega = 0.3$.

Figs. 2 show the effects on temperature graphs according to a change in different physical parameters. The effect of heat source/sink parameters, solutal stratification parameter S_t^*, Prandtl number Pr, thermal radiation parameter N_r, and Brownian motion N_b parameters are represented graphically. From Figs. 4.2 and 4.3, it can be seen that by growing the negative values of A^* and B^* the temperature profile decreases and increases respectively for all three types of fluids, i.e, (dilatant, viscous, and pseudo-plastic fluids). Extra heat is produced in the internal fluid which increases the temperature boundary layer thickness and eventually leads to an increase in the temperature profile. Physically, the negative values of A^* and B^* generally performs as heat absorption and positive values of A^* and B^* performs as heat generation. Fig. 4.4 and 4.5 reveal the effects of Brownian motion N_b and thermal radiation N_r, against thermal profile respectively. By rising these parameters, the temperature profile is observed to have increasing effects gradually for dilatant, viscous, and pseudo-plastic fluids. The temperature profile upsurges because of the improving standards of the thermal radiation parameter. When a high-level temperature difference is needed, we use thermal radiation. It is observed that an improvement in the radiation parameter provides more temperature to the fluid which indicates a boost in temperature. Fig. 4.6. outlined to reveals the impact of thermal stratification on the thermal field. This is noticed that fluid temperature is declining against the effect of thermal stratification with an upsurge in adjustable thickness parameter. The actual convective potential which co-exists between the non-uniform extending sheet and the ambient nanofluid reduced with a rise in S_t. In sight of this, the thermal boundary layer thickness and fluid temperature decreased for greater thermal

stratification. The rate of heat transfer at the sheet growths for an upsurge in the quantity of thermal layer.

Figs. 4.7-4.11 reveal the concentration graphs for diverse values of N_b, N_t, A^*, Sc, and S_t^* respectively. The rest of the parameters stay on fixed. Fig. 4.7 displays the variation of Brownian motion against the concentration of nanoparticles. It is seen that the concentration profile is decreasing by increment in Brownian motion parameter N_b. Fig. 4.8 shows the concentration profile with respect to increasing in thermophoresis parameter. It can be noticed that the concentration field is rising with respect to an enhancement in thermophoresis parameter N_t for all three cases of fluids. Fig. 4.9 represents the effect of heat absorption coefficient over the concentration profile. This reveals, the concentration profile is showing dual behavior by increasing the heat absorption parameter. The concentration profile increased near surface < 2, but this trend is the opposite in far field surface > 2. Fig. 4.10 demonstrates the influence of Schmidt number against the concentration profile. It is realized the concentration is decreasing against increasing in Sc. Fig. 4.11 represents an impression of solutal stratification on the concentration profile which discloses that as the values of S_t boosts, the concentration boundary layer thickness reduces gradually.

Figs. 4.12-4.18 show the graphical representation of motile microorganism function $H(\xi)$ with changing values of heat absorption parameters $A^*, B^* < 0$, Lewis number Le, Brownian motion parameter N_b, motile microbe parameter Ω, thermophoresis parameter N_t, and Peclet number Pe. Figs. 4.12-4.13 examine the variation in motile microorganisms against heat absorption parameters. The increasing behavior in $H(\xi)$ is seen with negative increments in thermal absorption parameters. Effect of Lewis number against the $H(\xi)$ is determined in Fig. 4.14. Which reveals the decreasing impact of $H(\xi)$ which referred to the increasing numerical values of Le. Substantially, while bioconvection Lewis number raises, then mass diffusivity of the nanofluid decreases, which facilitates to decrease the solute concentration, and finally, the motile microbe density declines. The effect of Brownian motion against microorganism profile graphically represented in Fig. 4.15. The Brownian motion is the random motion of the floating nanoparticles in the base fluid, and the molecules interchange extremely rapidly in the base fluid. Therefore, it is determined the declining profile of $H(\xi)$ for leading values of Brownian motion. The impression of thermophoresis is

shown against the $H(\xi)$ in Fig. 4.16 which examined, the boost up in $H(\xi)$ by leading values of thermophoresis parameters. In the thermophoresis procedure, tiny particles transfer from high region temperature to the low region temperature, which finally causes an enhancement in the fluid temperature. Fig. 4.17 demonstrates the influence of motile microbe parameter Ω over the concentration of microorganisms. Graphical results execute the declining change in $H(\xi)$ with respect to leading values of Ω. Fig. 4.18 predicts the graphical representation of Peclet number Pe with respect to microorganism profile. The ratio of maximum cell swimming speed to diffusion of microbes is denoted as Peclet number. Diffusion is the procedure by with a substance goes from an area of high-level concentration to an area of low-level concentration. It describes the progress of the elements in the fluid. It is observed that diffusivity of microbes is declined in the case of an expansion in Pe. The physical defenses of such reducing microorganism profile are because Peclet number is reversely fell on motile intensity.

Tables 4.1 determines the outcomes of non-dimensional parameters on skin friction. The effect of the R-P fluid parameter and variable thickness parameter are analyzed, while the rest of all parameters remained fix. An increment in the both parameters are observed to increase the drag friction.

Various parameters are examined on the Nusselt, Sherwood number, and density of motile microbes which are shown in table 4.2. It is noted, by increasing wall thickness and R-P fluid parameter the Nusselt, Sherwood number, and motile density of microbes are increasing numerically. Heat generation, thermal stratification, and Schmidth number are increasing the Sherwood number as well as density of microorganism's number but decreasing the Nusselt number. Solutal stratification and Prandtl number are analyzed to increasing the Nusselt number however decreasing for Sherwood and density of microbe's number. where Peclet number is seen to decrease the density of motile microbes.

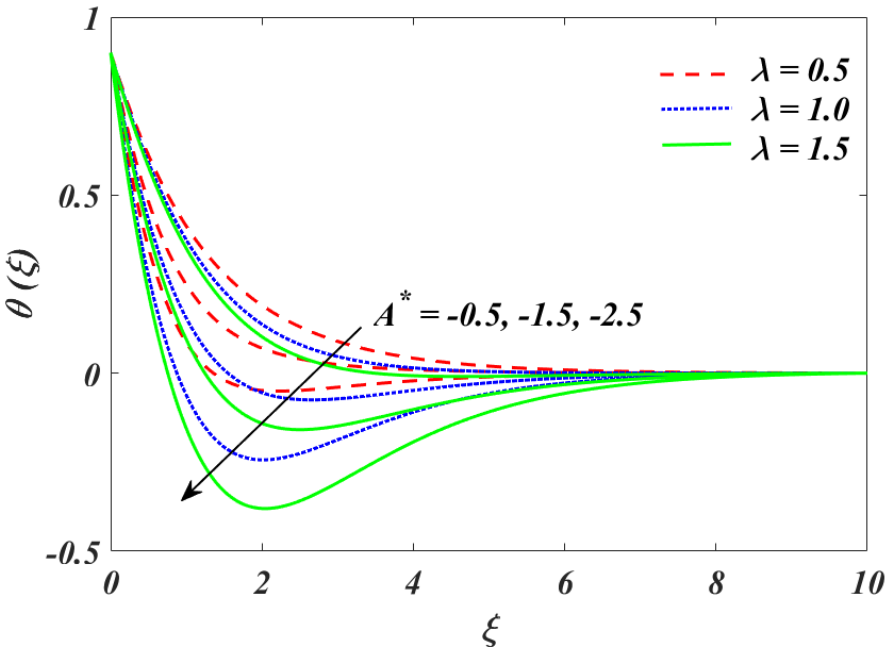

Fig. 4.2: Variation of A^* on $\theta(\xi)$.

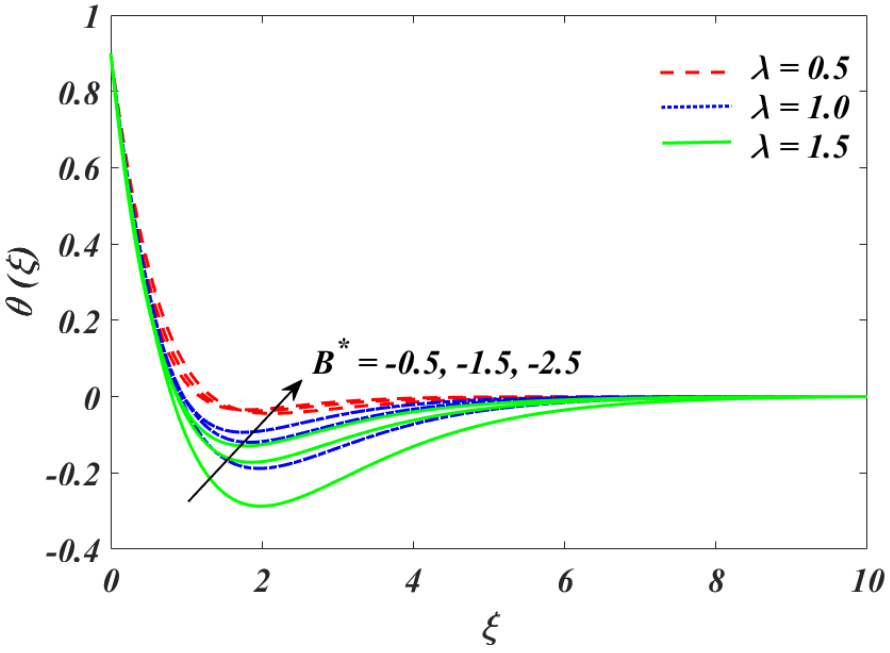

Fig. 4.3: Variation of B^* on $\theta(\xi)$.

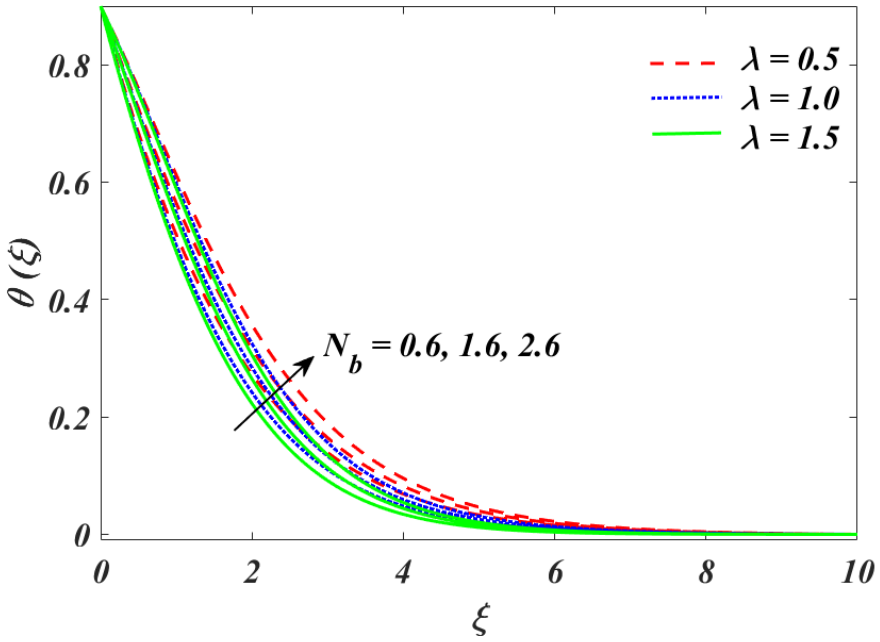

Fig. 4.4: Variation of N_b on $\theta(\xi)$.

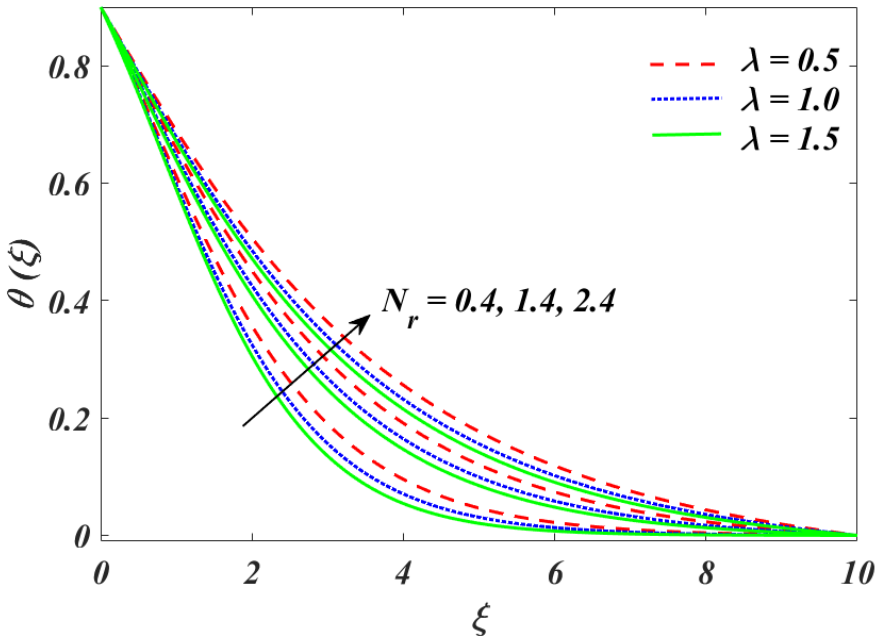

Fig. 4.5: Variation N_r of on $\theta(\xi)$.

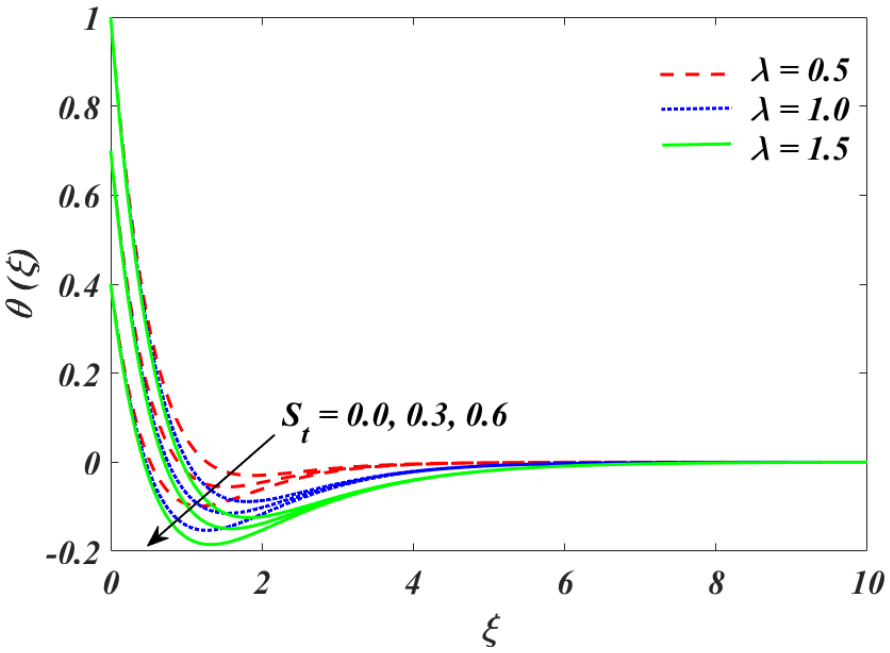

Fig.4.6: Variation of S_t on $\theta(\xi)$.

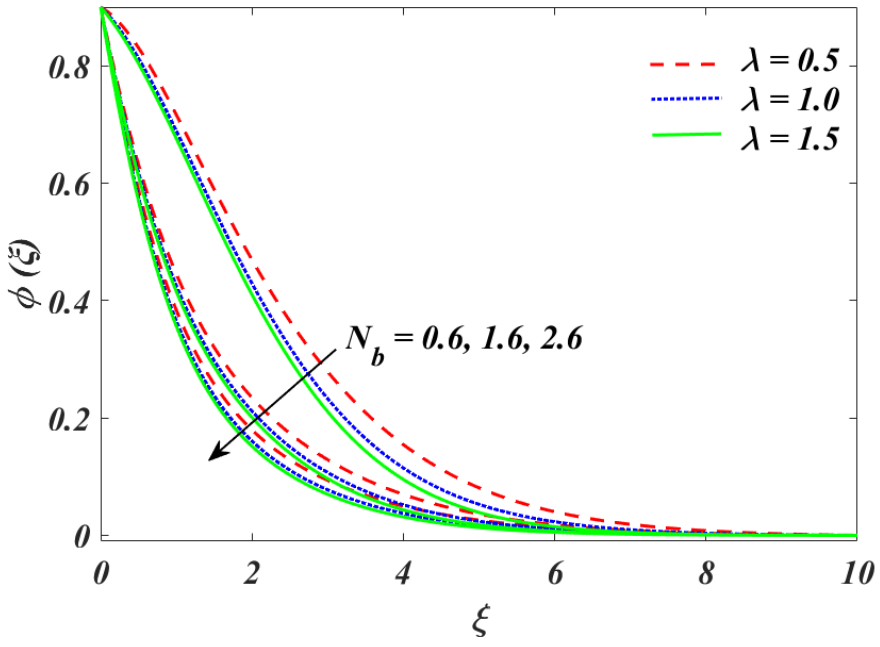

Fig. 4.7: Variation of N_b on $\phi(\xi)$.

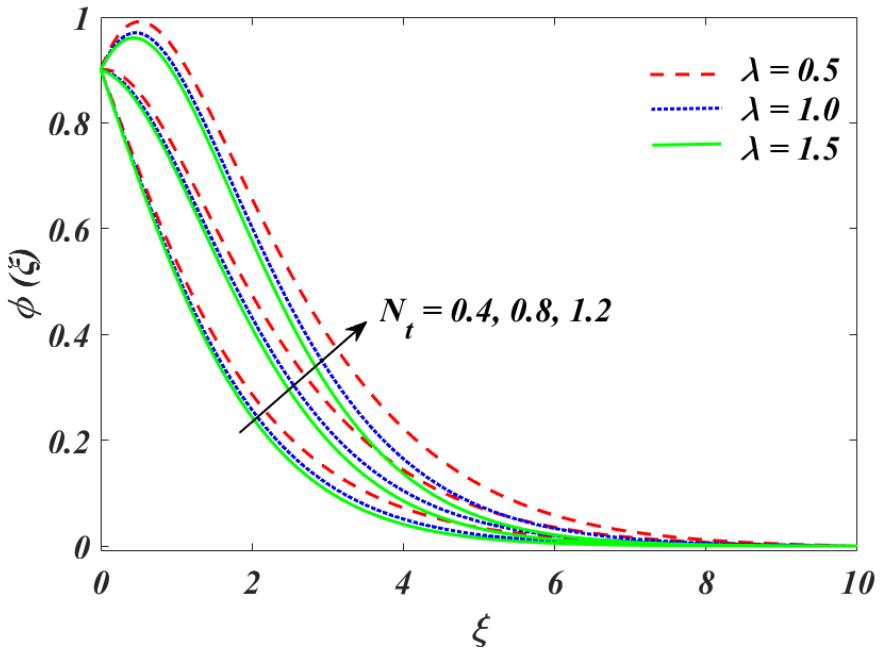

Fig. 4.8: Variation of N_t on $\phi(\xi)$.

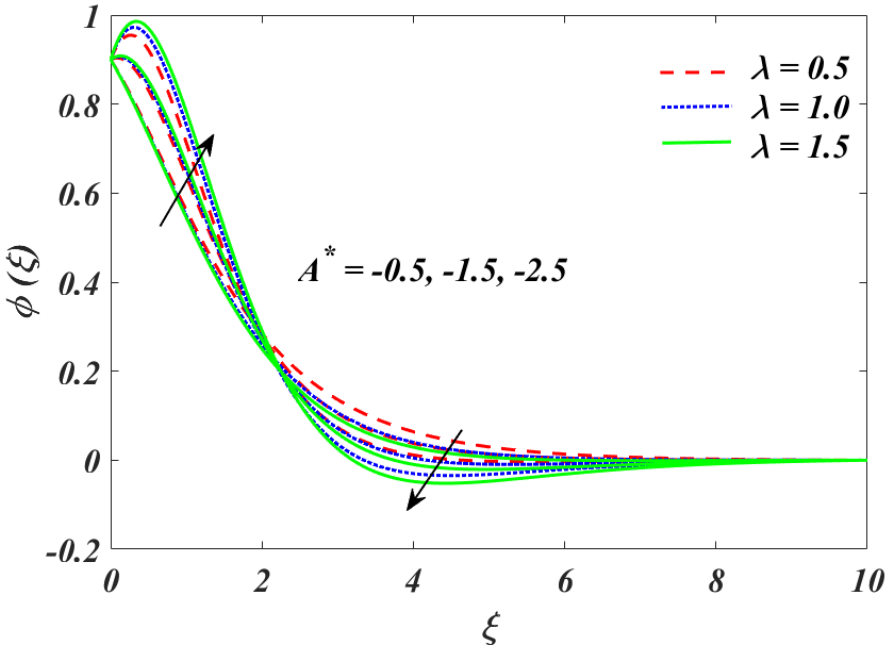

Fig. 4.9: Variation of A^*on $\phi(\xi)$.

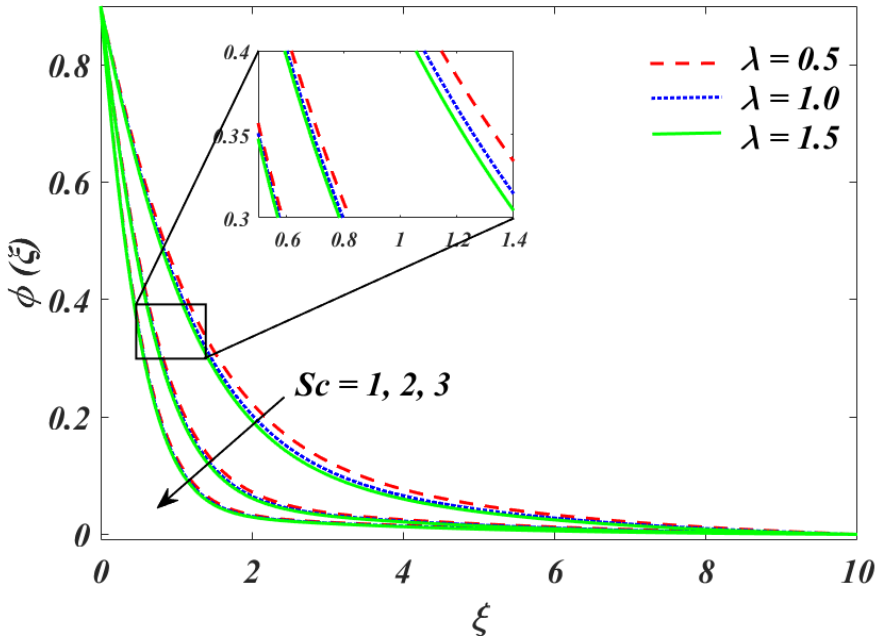

Fig. 4.10: Variation of Sc on $\phi(\xi)$.

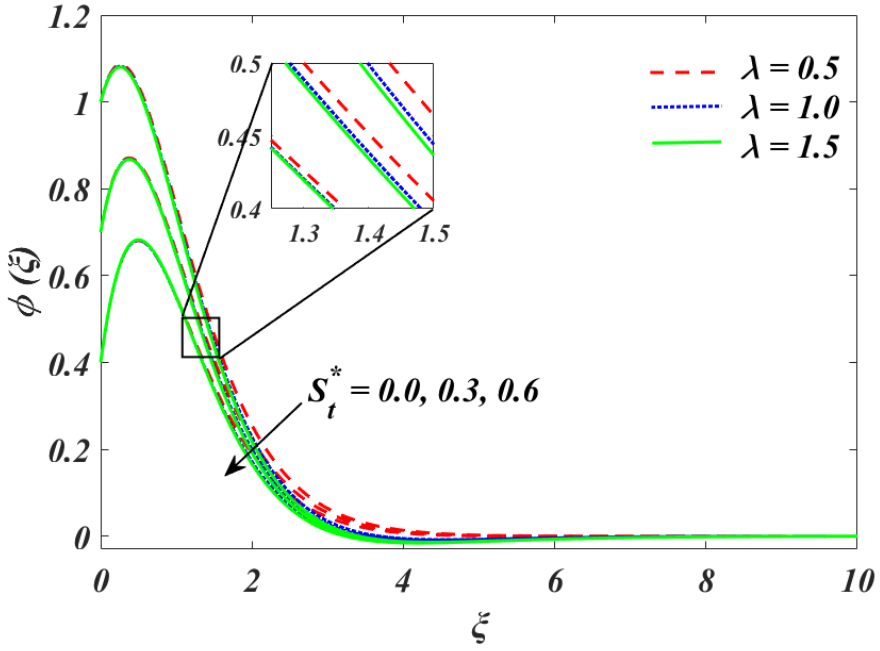

Fig. 4.11: Variation of S_t^* on $\phi(\xi)$.

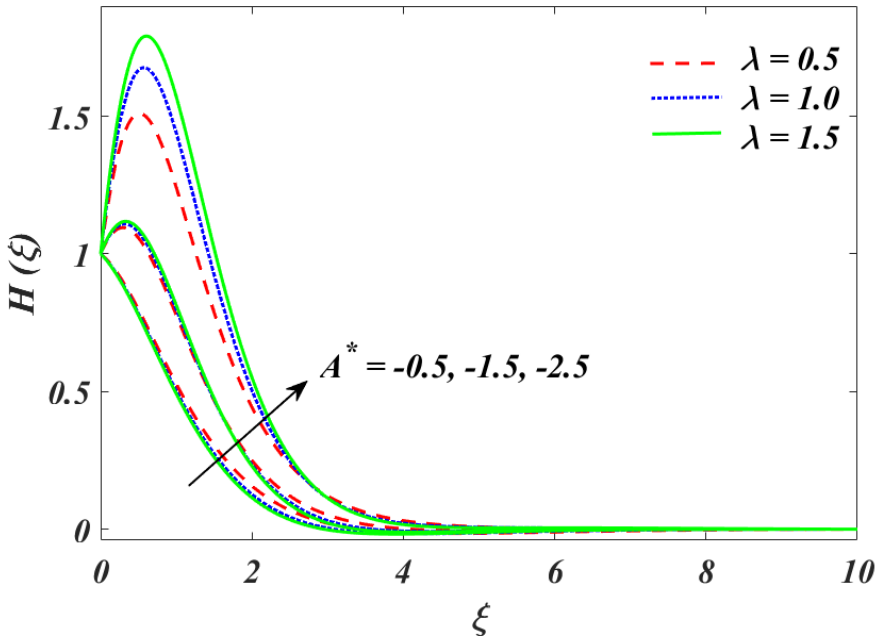

Fig. 4.12: Variation of A^*on $H(\xi)$.

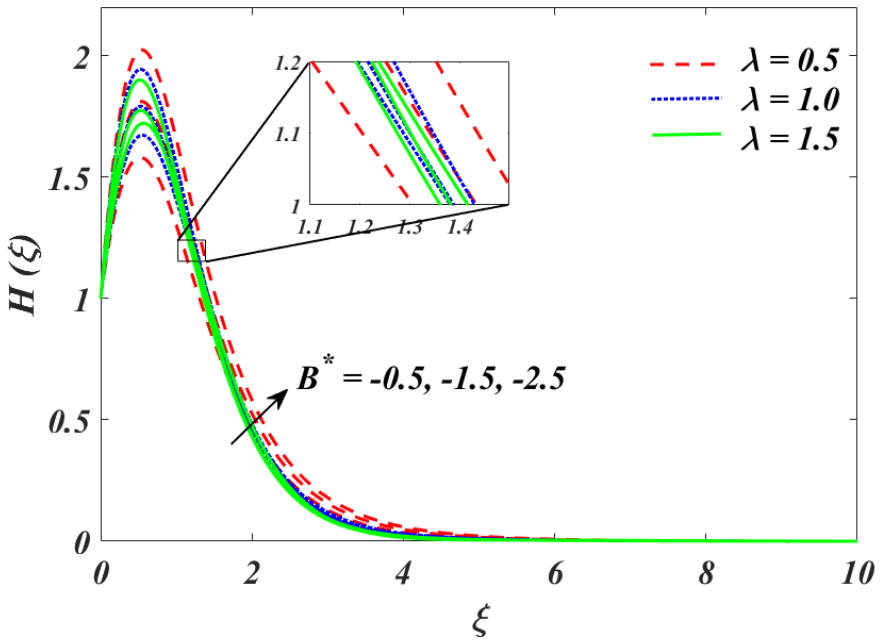

Fig. 4.13: Variation of B^* on $H(\xi)$.

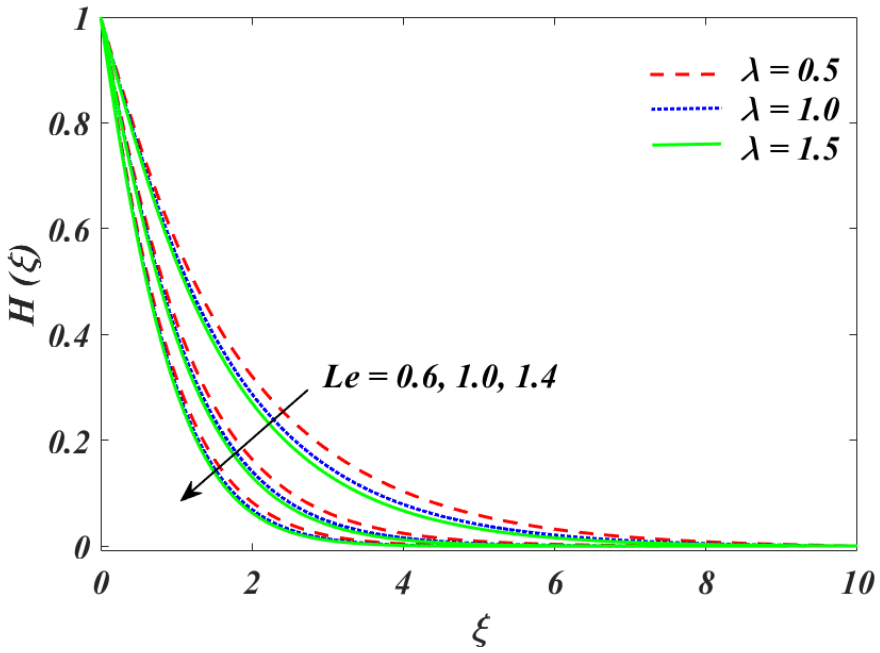

Fig. 4.14: Variation of Le on $H(\xi)$.

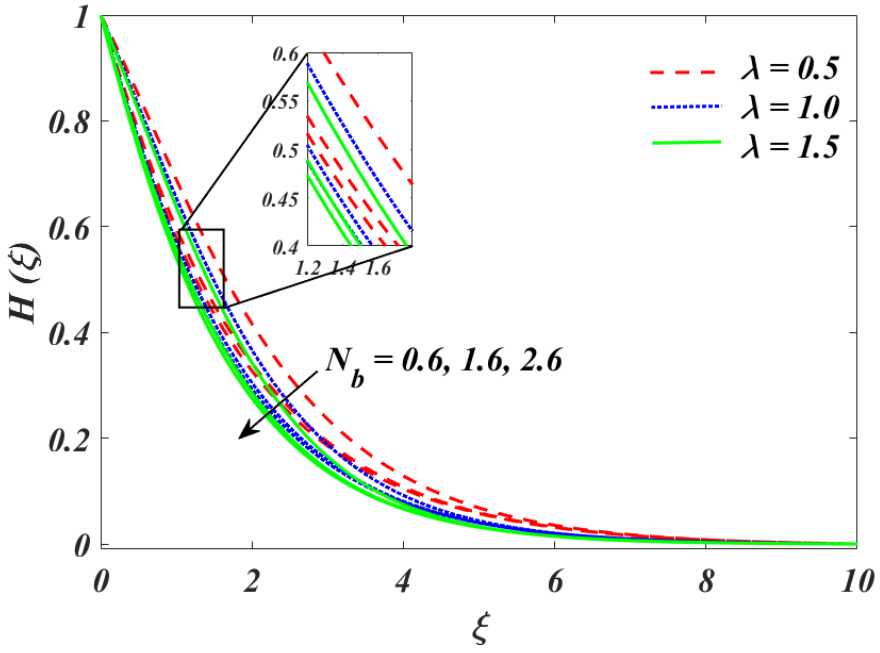

Fig. 4.15: Variation of N_b on $H(\xi)$.

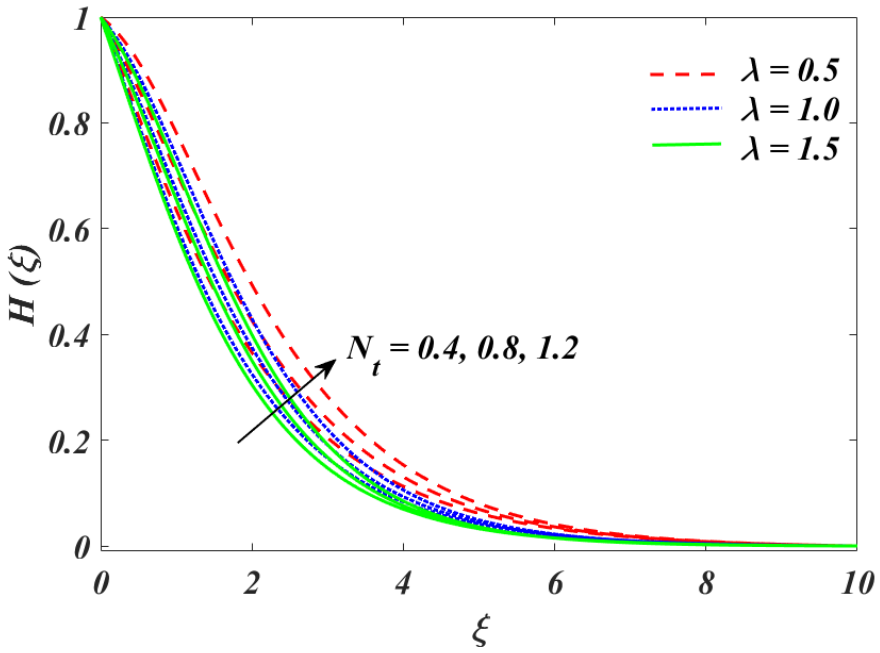

Fig. 4.16: Variation of N_t on $H(\xi)$.

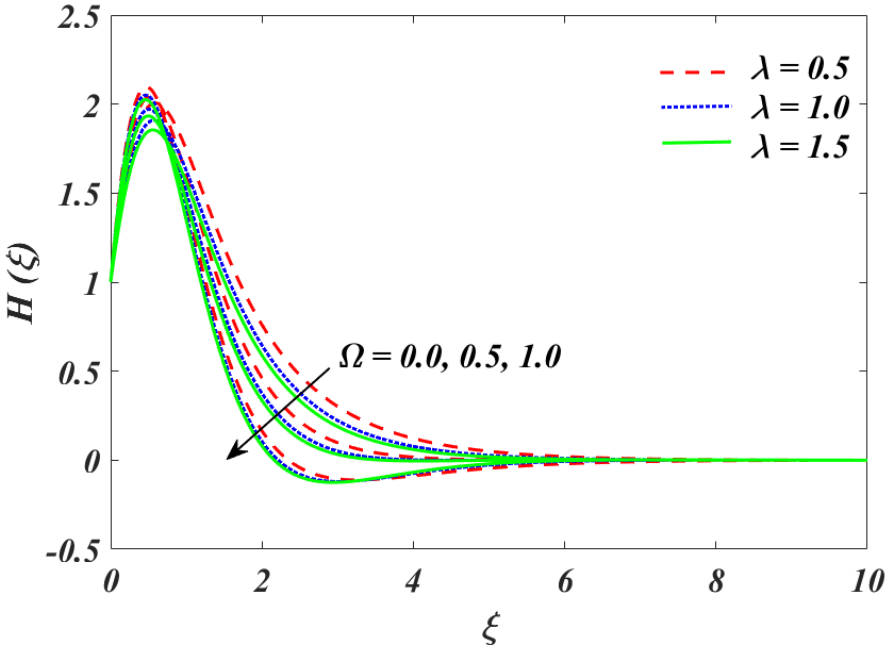

Fig. 4.17: Variation of Ω on $H(\xi)$.

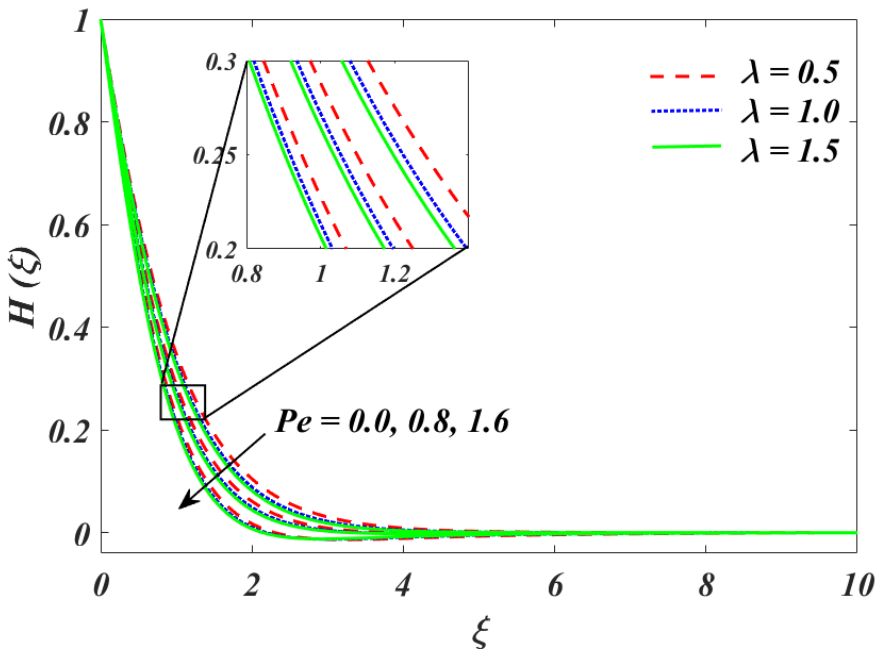

Fig. 4.18: Variation of Pe on $H(\xi)$.

Table 4.1: Impact of α and λ on C_{fx} with $, N_t = N_b = Pe = N_r = 0.4,\ Le = \Omega = Pr = Sc = 1,$ $A^* = B^* = -0.2, S_t = S_t^* = 0.1, \gamma = 0.5.$

α	λ	$-C_{fx}$
0	0.5	0.571308
0.4		0.656306
0.8		0.747033
1.2	0.5	0.842699
	0.6	0.859842
	1	0.917018
	1.4	0.962575

Table 4.2: Impact of different parameters on $-Nu_x$ $-Sh_x$ $-Nn_x$ with $\gamma = 0.5$, $N_t = N_b = N_r = 0.4$, $Le = \Omega = 1$.

α	λ	Pr	Pe	Sc	A^*	B^*	S_t	S_t^*	$-Nu_x$	$-Sh_x$	$-Nn_x$
0	0.5	1	0.4	1	0.1	0.1	0.1	0.1	0.092664	0.459379	0.520150
0.4									0.177457	0.479695	0.631975
0.8									0.266544	0.501700	0.748172
1.2	0.5								0.358084	0.526677	0.868694
	0.6								0.369834	0.531806	0.875527
	1								0.399789	0.550113	0.894032
	1.4	1							0.415777	0.564660	0.905318
		2							0.694294	0.422640	0.836402
		4							0.896694	0.319405	0.778628
		6	0.4						0.982400	0.275610	0.752348
			0.6						0.982400	0.275610	0.745945
			0.8						0.982400	0.275610	0.743710
			1.0	1					0.982400	0.275610	0.746638
				2					0.878658	0.889416	1.494834
				3					0.829394	1.402319	2.164826
				4	0.1				0.800025	1.870980	2.792887
					0.3				0.755582	1.893986	2.822448
					0.5				0.710885	1.917129	2.852043
					0.7	0.1			0.665931	1.940413	2.881675
						0.3			0.624120	1.962395	2.909770
						0.5			0.580128	1.985382	2.938718
						0.7	0.1		0.533575	2.009543	2.968664
							0.2		0.523062	2.041250	2.993758
							0.4		0.494379	2.108016	3.046067
							0.6	0.1	0.455204	2.179437	3.101223
								0.2	0.473761	1.961786	2.873849
								0.4	0.512860	1.525247	2.388890
								0.6	0.554711	1.086986	1.857670

CHAPTER 5

CONCLUSION

This chapter consists of the summary and final remarks of the problem are discussed in chapter 3 and chapter 4. Different parameters are showing several effects on concentration, velocity profile in the presence of transverse MHD flow exceeding the non-linear stretched sheet with variable thickness which have been represented graphically in previous chapters. The conclusion of both problems are as follows:

5.1 Concluding Remarks

Chapter 3 investigated the characteristics of nonlinearly stretched sheet having variable thickness on the Reiner-Philippoff fluid flow which is the classical model of non-Newtonian fluid. The solution of the relative boundary-layer equation is attained to determine the effect of irregular surface considering the R-P flow. Suitable transformation along with stretched velocity are under consideration for BVP.

- The thickness of surface and nature of fluid of the type (viscous, dilatant or pseudo-plastic) considerably alter the characteristics of flow.
- The thickness of the surface is useful to control the skin friction and velocity profile.
- The rate of change of drag friction according to Bingham number is observed to be positive for dilatant fluid, negative for pseudo-plastic and zero for viscous fluid.

The related work contains a innovative study of Reiner–Philippoff nanofluid flow in the attendance of gyrotactic microbe over a slandering sheet, which is quite interesting the inclusion of gyrotactic microorganism. Thermal radiation and double stratification are also considered in the energy equation. To obtain numerical solution, mathematical behavior is

carried out via shooting technique and RK method by using computational software MATLAB. The major outcomes may be expressed as:

- The growth in heat absorption parameters tends to dual behavior of increasing nearby the surface and declining for the surface of energy and concentration profiles.
- The temperature profile is improving by rising the values of $N_r, N_b,$ and B^*, and declining by leading values of S_t.
- The augmentation in N_t is accelerating the concentration profile. However, concentration is decreasing by leading values of A^*, N_b, Sc, and S_t.
- The motile density of microorganism profile $H(\xi)$ is depreciates on the rising change of $\Omega,$ and N_b. While the increments N_t, A^*, and B^* causing the improving in density of microorganisms.
- The density of motile microbe is reducing by enhancing bioconvection Lewis number and Peclet number.
- The amount of skin friction is boosting up with expanding wall thickness and Reiner-Philippoff parameter.
- Nusselt, Sherwood, and density motile organism are to be control by varying wall thickness parameter.

REFERENCES

1. Ahmad, A., M. Qasim, and S. Ahmed, *Flow of Reiner–Philippoff fluid over a stretching sheet with variable thickness.* Journal of the Brazilian Society of Mechanical Sciences and Engineering, 2017. **39**(11): p. 4469-4473.
2. Kumar, K.G., et al., *Cattaneo–Christov heat diffusion phenomenon in Reiner–Philippoff fluid through a transverse magnetic field*. Physica A: Statistical Mechanics and its Applications, 2020. **541**.
3. Sajid, T., T. Sagheer, and S. Hussain, *Impact of Temperature-Dependent Heat Source/Sink and Variable Species Diffusivity on Radiative Reiner–Philippoff Fluid.* Mathematical Problems in Engineering, 2020. **2020**(9701860): p. 1-16.
4. Na, T.Y., *BOUNDARY LAYER FLOW OF REINER-PHILIPPOFF FLUIDS.* Pergamon, 1994: p. 1-7.
5. Ahmad, A., *Flow of ReinerPhilippoff based nano-fluid past a stretching sheet.* Journal of Molecular Liquids, 2016. **219**: p. 643-646.
6. Tahir, M. and A. Ahmad, *Impact of pseudoplaticity and dilatancy of fluid on peristaltic flow and heat transfer: Reiner-Philippoff fluid model.* Advances in Mechanical Engineering, 2020. **12**(12).
7. Gnaneswara Reddy, M., et al., *Physical aspects of Darcy–Forchheimer flow and dissipative heat transfer of Reiner–Philippoff fluid.* Journal of Thermal Analysis and Calorimetry, 2019. **141**(2): p. 829-838.
8. Khan, S.U., K. Al-Khaled, and M.M. Bhatti, *Numerical experiment of Reiner–Philippoff nanofluid flow subject to the higher-order slip features, activation energy, and bioconvection.* Partial Differential Equations in Applied Mathematics, 2021. **4**.
9. Li, Y.-X., et al., *Study of radiative Reiner–Philippoff nanofluid model with gyrotactic microorganisms and activation energy: A Cattaneo–Christov Double Diffusion (CCDD) model analysis.* Chinese Journal of Physics, 2021. **73**: p. 569-580.
10. Ahmad, S., M. Ashraf, and K. Ali, *Bioconvection due to gyrotactic microbes in a nanofluid flow through a porous medium.* Heliyon, 2020. **6**(12): p. e05832.

11. Chu, Y.-M., et al., *Significance of activation energy, bio-convection and magnetohydrodynamic in flow of third grade fluid (non-Newtonian) towards stretched surface: A Buongiorno model analysis.* International Communications in Heat and Mass Transfer, 2020. **118**.
12. Reddy, M.G., et al., *Transverse magnetic flow over a Reiner–Philippoff nanofluid by considering solar radiation.* Modern Physics Letters B, 2019. **33**(36).
13. Gopal, D., et al., *The impact of thermal stratification and heat generation/absorption on MHD carreau nano fluid flow over a permeable cylinder.* SN Applied Sciences, 2020. **2**(4).
14. Srinivasacharya, D. and M. Upendar, *Effect of double stratification on MHD free convection in a micropolar fluid.* Journal of the Egyptian Mathematical Society, 2013. **21**(3): p. 370-378.
15. Srinivasacharya, D. and O. Surender, *Effect of double stratification on mixed convection boundary layer flow of a nanofluid past a vertical plate in a porous medium.* Applied Nanoscience, 2014. **5**(1): p. 29-38.
16. Salah, F., et al., *Thermal stratification effects on MHD radiative flow of nanofluid over nonlinear stretching sheet with variable thickness.* Journal of Computational Design and Engineering, 2018. **5**(2): p. 232-242.
17. Rehman, K.U., et al., *Temperature and concentration stratification effects on non-Newtonian fluid flow past a cylindrical surface.* Results in Physics, 2017. **7**: p. 3659-3667.
18. Ibrahim, W. and O.D. Makinde, *The effect of double stratification on boundary-layer flow and heat transfer of nanofluid over a vertical plate.* Computers & Fluids, 2013. **86**: p. 433-441.
19. Chung, J.D., et al., *Partially ionized hybrid nanofluid flow with thermal stratification.* Journal of Materials Research and Technology, 2021. **11**: p. 1457-1468.
20. Shah, Z., et al., *Impact of Nonlinear Thermal Radiation on MHD Nanofluid Thin Film Flow over a Horizontally Rotating Disk.* Applied Sciences, 2019. **9**(8).
21. Sajid, T., et al., *Impact of oxytactic microorganisms and variable species diffusivity on blood-gold Reiner–Philippoff nanofluid.* Applied Nanoscience, 2020. **11**(1): p. 321-333.

22. Raju, C.S.K., et al., *Cross diffusion effects on magnetohydrodynamic slip flow of Carreau liquid over a slendering sheet with non-uniform heat source/sink.* Journal of the Brazilian Society of Mechanical Sciences and Engineering, 2018. **40**(4).
23. Qayyum, S., T. Hayat, and A. Alsaedi, *Chemical reaction and heat generation/absorption aspects in MHD nonlinear convective flow of third grade nanofluid over a nonlinear stretching sheet with variable thickness.* Results in Physics, 2017. **7**: p. 2752-2761.
24. Ahmed, A., et al., *Thermal analysis in unsteady radiative Maxwell nanofluid flow subject to heat source/sink.* Applied Nanoscience, 2020. **10**(12): p. 5489-5497.
25. Sajid, T., et al., *Impact of double-diffusive convection and motile gyrotactic microorganisms on magnetohydrodynamics bioconvection tangent hyperbolic nanofluid.* Open Physics, 2020. **18**(1): p. 74-88.
26. Sajid, T., M. Sagheer, and S. Hussain, *Impact of Temperature-Dependent Heat Source/Sink and Variable Species Diffusivity on Radiative Reiner–Philippoff Fluid.* Mathematical Problems in Engineering, 2020. **2020**: p. 1-16.
27. Hayat, T., et al., *MHD flow of Powell-Eyring nanofluid over a non-linear stretching sheet with variable thickness.* Results in Physics, 2017. **7**: p. 189-196.
28. Hayat, T., et al., *Modern aspects of nonlinear convection and magnetic field in flow of thixotropic nanofluid over a nonlinear stretching sheet with variable thickness.* Physica B: Condensed Matter, 2018. **537**: p. 267-276.
29. Ullah, K., et al., *Heat transfer analysis based on cattaneo-christov heat flux model and convective boundary conditions for flow over an oscillatory stretching surface.* Thermal Science, 2017(00): p. 172-172.
30. Alam, A., D.N.K. Marwat, and A. Ali, *Flow of nano-fluid over a sheet of variable thickness with non-uniform stretching (shrinking) and porous velocities.* Advances in Mechanical Engineering, 2021. **13**(4).
31. Cortell, R., *Heat and fluid flow due to non-linearly stretching surfaces.* Applied Mathematics and Computation, 2011. **217**(19): p. 7564-7572.
32. Khashi'ie, N.S., et al., *Magnetohydrodynamic and viscous dissipation effects on radiative heat transfer of non-Newtonian fluid flow past a nonlinearly shrinking sheet: Reiner–Philippoff model.* Alexandria Engineering Journal, 2022.

33. Xiong, P.-Y., et al., *Entropy optimized Darcy-Forchheimer flow of Reiner-Philippoff fluid with chemical reaction.* Computational and Theoretical Chemistry, 2021. **1200**.
34. Pal, D. and S.K. Mondal, *Computational analysis of bioconvective flow of nanofluid containing gyrotactic microorganisms over a nonlinear stretching sheet with variable viscosity using HAM.* Journal of Computational Design and Engineering, 2020. **7**(2): p. 251-267.
35. Hatami, M. and D. Jing, *Peristaltic Carreau-Yasuda nanofluid flow and mixed heat transfer analysis in an asymmetric vertical and tapered wavy wall channel.* Reports in Mechanical Engineering, 2020. **1**(1): p. 128-140.
36. Aziz, W.A.Khan.A., *Natural convection flow of a nanofluid over a vertical plate with uniform surface heat flux.* International Journal of Thermal Sciences, 2011. **50**: p. 1207-1214.
37. Hayat, T., et al., *Magnetohydrodynamic (MHD) nonlinear convective flow of Walters-B nanofluid over a nonlinear stretching sheet with variable thickness.* International Journal of Heat and Mass Transfer, 2017. **110**: p. 506-514.

BIOCONVECTION IN REINER-PHILIPPOFF FLUID FLOW OVER A SLENDERING SHEET

ORIGINALITY REPORT

18%	9%	14%	4%
SIMILARITY INDEX	INTERNET SOURCES	PUBLICATIONS	STUDENT PAPERS

PRIMARY SOURCES

1	Submitted to Higher Education Commission Pakistan Student Paper	3%
2	A. Ahmad, M. Qasim, S. Ahmed. "Flow of Reiner–Philippoff fluid over a stretching sheet with variable thickness", Journal of the Brazilian Society of Mechanical Sciences and Engineering, 2017 Publication	2%
3	www.hindawi.com Internet Source	1%
4	worldwidescience.org Internet Source	1%
5	link.springer.com Internet Source	1%
6	C. S. K. Raju, M. M. Hoque, P. Priyadharshini, B. Mahanthesh, B. J. Gireesha. "Cross diffusion effects on magnetohydrodynamic slip flow of Carreau liquid over a slendering	1%